UCRL-1908

c.2

UNCLASSIFIED

UNIVERSITY OF CALIFORNIA — BERKELEY

TWO-WEEK LOAN COPY

This is a Library Circulating Copy which may be borrowed for two weeks. For a personal retention copy, call Tech. Info. Division, Ext. 5545

RADIATION LABORATORY

UCRL-1908 c.2

DISCLAIMER

This document was prepared as an account of work sponsored by the United States Government. While this document is believed to contain correct information, neither the United States Government nor any agency thereof, nor the Regents of the University of California, nor any of their employees, makes any warranty, express or implied, or assumes any legal responsibility for the accuracy, completeness, or usefulness of any information, apparatus, product, or process disclosed, or represents that its use would not infringe privately owned rights. Reference herein to any specific commercial product, process, or service by its trade name, trademark, manufacturer, or otherwise, does not necessarily constitute or imply its endorsement, recommendation, or favoring by the United States Government or any agency thereof, or the Regents of the University of California. The views and opinions of authors expressed herein do not necessarily state or reflect those of the United States Government or any agency thereof or the Regents of the University of California.

UCRL-1908
Unclassified-Chemistry Distribution

UNIVERSITY OF CALIFORNIA

Radiation Laboratory

Contract No. W-7405-eng-48

CRYSTAL STRUCTURES OF SODIUM SUPEROXIDE AND YTTRIUM TRICHLORIDE

G. F. Carter
(Thesis)

August, 1952

Berkeley, California

TABLE OF CONTENTS

Page

ABSTRACT 3

CHAPTER I. LOW TEMPERATURE CRYSTAL STRUCTURES OF SODIUM SUPEROXIDE

I. INTRODUCTION. 5

II. APPARATUS 6

III. NaO_2-II: PYRITE STRUCTURE. 8

IV. NaO_2-III: MARCASITE STRUCTURE. 9

V. KO_2-I: CRYSTAL STRUCTURE 13

VI. INTERPRETATION OF RESULTS 14

CHAPTER II. CRYSTAL STRUCTURE OF YTTRIUM TRICHLORIDE

I. INTRODUCTION. 16

II. EXPERIMENTAL PROCEDURE. 16

A. Preparation of Yttrium Trichloride 16

B. Unit Cell. 17

III. TRIAL STRUCTURE 18

IV. ANALYSIS OF STRUCTURE 21

V. DISCUSSION OF STRUCTURE 25

VI. ISOSTRUCTURAL RARE EARTH TRICHLORIDES 29

VII. ACKNOWLEDGMENT. 31

VIII. REFERENCES. 32

IX. TABLES. 34

X. FIGURES 59

CRYSTAL STRUCTURES OF SODIUM SUPEROXIDE
AND YTTRIUM TRICHLORIDE

Giles F. Carter
Department of Chemistry and Radiation Laboratory
University of California, Berkeley, California

September 1952

ABSTRACT

Crystal structures of two low temperature forms of sodium superoxide have been deduced from Debye-Scherrer powder diffraction patterns and Weissenberg equi-inclination photographs. Apparatus for taking x-ray diffraction patterns at low temperatures over a range from room temperature to 100° K was constructed. Two rapid, reversible transitions were found to occur at -50° C and -77° C; NaO_2-II, stable between -50° C and -77° C, has a pyrite-type structure with space group T_h^6-Pa3 and lattice constant $\underline{a}$ = 5.48 A. After single crystals had been grown from a solution of NaO_2 in liquid ammonia, the structure of NaO_2-III was found to be orthorhombic (space group D_{2h}^{12}--Pnnm) with lattice constants $\underline{a}$ = 4.26 A, $\underline{b}$ = 5.54 A, $\underline{c}$ = 3.44 A. Parameters of oxygen atoms were chosen primarily on the basis of geometrical arguments for most economical packing, and these agreed with parameters found upon calculation of an electron density section using data from the powder pattern. A close comparison exists between the structures of NaO_2-II and pyrite and likewise between NaO_2-III and marcasite (also FeS_2).

The crystal structure of yttrium trichloride, deduced from single-crystal, equi-inclination Weissenberg photographs, indicates a monoclinic unit cell: $\underline{\beta}$ = $110^{\circ}20'$, $\underline{a}$ = 6.92 A, $\underline{b}$ = 11.94 A,

c = 6.44 A; the structure, having the space group C_{2h}^{3}--C2/m, consists roughly of six layers of atoms stacked in planes perpendicular to the b axis. The arrangement of chlorine atoms is such that they approximate a face-centered cubic, closest packing of spheres. Each yttrium atom has three closest yttrium neighbors at a distance of 4.0 A and six nearest chlorine neighbors at 2.65 A; chlorine atoms each have twelve chlorine neighbors at distances varying between 3.54 A and 4.38 A. Dysprosium, holmium, erbium, thulium, ytterbium, and lutecium trichlorides are isostructural with yttrium trichloride, and lattice parameters for those compounds were obtained from x-ray diffraction powder patterns.

CRYSTAL STRUCTURES OF SODIUM SUPEROXIDE AND YTTRIUM TRICHLORIDE

Giles F. Carter
Department of Chemistry and Radiation Laboratory
University of California, Berkeley, California

September 1952

LOW TEMPERATURE CRYSTAL STRUCTURES OF SODIUM SUPEROXIDE

I. INTRODUCTION

Superoxides of potassium, rubidium, and cesium may be formed from reaction of the elements.[1-3] Evidence for the existence of sodium superoxide was first indicated by the appearance of a yellow color in a solution of liquid ammonia in which metallic sodium had been oxidized.[4] Sizeable quantities of the superoxide were found obtainable in reasonably pure form by reaction of sodium peroxide with oxygen at approximately 500° C and 300 atmospheres pressure.[5] At room temperature the crystal structure of sodium superoxide is face-centered cubic, NaCl type, with the superoxide ions occupying halide positions with disordered orientations.[6] In order for the lattice to be face-centered, the superoxide groups must have some kind of disordered orientation; four sets of oxygen positions have been proposed: (1) the pair rotates freely; (2) the pair is oriented parallel to one of the three cubic axes; (3) the pair is parallel to one of the six face diagonals; (4) the pair is parallel to one of the four body diagonals.[6] However, a definite choice between these structures was impossible since the agreement between observed and calculated intensities was reasonably good in all four cases.

The existence of disorder in the structure of sodium superoxide at room temperature suggested a low temperature transformation in which sodium superoxide would undergo a change in structure.[6] A study of two low temperature structures of this compound, by means of x-ray diffraction methods, is described in this paper. Both Debye-Scherrer powder patterns and Weissenberg equi-inclination photographs of single crystals were used.

The entire problem required (1) construction of an x-ray diffraction camera suitable for taking powder patterns at low temperatures and adaptation of the Weissenberg camera for taking pictures of samples below room temperature, (2) the determination of the experimental technique for actually taking low temperature diffraction patterns, (3) the deduction of the crystal structures discovered as a result of investigations carried out with the low temperature camera, and (4) the interpretation of the results of these crystal structures.

Hereafter the room temperature form of sodium superoxide will be referred to as NaO_2-I; NaO_2-I is stable apparently from high temperatures to about -50° C, where it undergoes a transformation to NaO_2-II, having a pyrite, FeS_2, structure.[7] This modification of NaO_2 is stable in a region from -50° C to -77° C, where it transforms to NaO_2-III, having a structure similar to that of marcasite, a polymorphic modification of FeS_2.[8,9]

II. APPARATUS

The source for obtaining low temperatures while exposing x-ray diffraction patterns was liquid nitrogen stored in a Dewar flask.

Cold nitrogen gas was blown through cellophane tubes over the sample; the amount of nitrogen blown over the sample was regulated by boiling the nitrogen at different rates, the rate of boiling being controlled by the amount of current passing through a small heating unit inserted in the Dewar flask. Temperatures from room temperature to within fifteen degrees of the boiling point of liquid nitrogen (i.e. to about 95° K) were attainable, and all temperatures were measured by a chromel-alumel thermocouple inserted within the cellophane tubes close to the sample. Two cellophane tubes were used, the cold nitrogen passing through the inside of the small inner tube, then recirculating between the inner and outer tubes; in this way the inner tube was insulated and protected from the formation of frost. A stream of air was constantly blown over the surface of the outer tube to reduce the formation of frost; at all but the lowest temperatures attainable the interference of frost was negligible.

Powder diffraction patterns were obtained for both low temperature forms of NaO_2, but only the pattern of the intermediate form having the pyrite structure was indexed immediately. At first, several attempts to attain single crystals were made by fusing NaO_2 and cooling slowly; however, in every case the NaO_2 decomposed. Hence a method of growing NaO_2 crystals from solution was attempted, and it proved successful. A small amount of NaO_2 was dissolved in liquid ammonia at -33° C, and the ammonia was allowed to evaporate slowly, leaving tiny cubic crystals (about 0.1 to 0.3 millimeters on an edge) of NaO_2-I on the walls of the glass vessel. These were transferred to a dry box having an atmosphere of argon dried with

molten sodium, and in the dry box the crystals were removed and transferred to glass capillaries. The crystals were then suitable for a series of low temperature Weissenberg photographs to be taken.

The apparatus used in taking low temperature Weissenberg photographs was similar to that used in taking powder diffraction patterns; however, instead of using two cellophane tubes to surround the sample, no cellophane tubes were used. Instead, the cold nitrogen gas flowed through a tube having a large diameter (7 mm as compared to a 2.5 mm diameter tube in the apparatus described above); this stream of gas was reflected from the base of the sample in order to reduce the formation of frost on the capillary and also to prevent excessive condensation of moisture on the goniometer head. A liberal coating of oil also was used to prevent any possible rusting of the goniometer head due to condensation of water. Since the Dewar could not be placed very close to the sample, the cold nitrogen was blown through a 25 cm glass tube insulated with Santocel.

III. NaO_2-II: PYRITE STRUCTURE

In the powder diffraction pattern of NaO_2 cooled below -50° C other lines than those found in patterns of NaO_2-I appeared, indicating a primitive rather than face-centered cubic symmetry. Observed intensities were estimated visually by comparing the lines obtained on a diffraction pattern of NaO_2-II with a film having various exposures of known intensities. Intensities were calculated for NaO_2 in the pyrite type structure by Templeton and Dauben,[6] with the oxygen parameter chosen as 0.438.

The data obtained from the powder pattern and these calculated intensities appear in Table I. The agreement between calculated and observed intensities shows this new form to have a pyrite structure. The space group is T_h^6-Pa3 with $\underline{a}$ = 5.48 ± 0.01 A; the sodium atoms are in 4(b) positions:[10] 000; 0, 1/2, 1/2; 1/2, 0, 1/2; 1/2, 1/2, 0, and the oxygen atoms are in 8(h) positions: ± (uuu; u + 1/2, 1/2 - u, u; - u, u + 1/2, 1/2 - u; 1/2 - u, - u, u + 1/2) with u = 0.439. The O--O distance is taken from the structure of NaO_2-I[6] to be 1.35 A, and the Na--O distance is 2.41 A. A discrepancy of 18.1 percent between observed and calculated intensities (not structure factors) was obtained from the equation

$$D = \frac{\Sigma \left| I_{obs.} - I_{calc.} \right| \cdot 100}{\Sigma \; I_{obs.}} .$$

Subsequent to the discovery of the pyrite structure of sodium superoxide, specific heat measurements[11] indicated transitions at -50° C and at -77° C; these may be interpreted as the transitions from the room temperature, disordered sodium chloride structure to the low temperature pyrite structure, and from the pyrite structure to the low temperature marcasite structure respectively.

IV. NaO_2-III: MARCASITE STRUCTURE

With the apparatus previously described equi-inclination Weissenberg photographs of twinned crystals of NaO_2-III were taken of the zero and first layer lines. These twinned crystals always resulted when single crystals of NaO_2-I were cooled below -77° C. Though the axis of rotation was a body diagonal of the unit cell,

the orthorhombic structure of NaO_2-III was deduced from this series of photographs.

The space group of NaO_2-III is D_{2h}^{12}--Pnnm, and the structure is similar to that of marcasite, FeS_2.[8,9] The lattice constants are $\underline{a}$ = 4.26 A, $\underline{b}$ = 5.54 A, and $\underline{c}$ = 3.44 A. There are two molecules per unit cell with sodium atoms at 2(a) positions:[10] 000 and 1/2, 1/2, 1/2; oxygen atoms are at 4(g) positions: $\pm$ (uv0; 1/2 - u, v + 1/2, 1/2), with u = 0.119 and v = 0.420. These parameters were chosen primarily on the basis of geometrical arguments for most economical packing with the O--O distance assumed to be 1.35 A. The data from the Weissenberg photographs were too poor to be useful for the determination of the parameters listed above. Data from the powder diffraction pattern gave only a broad peak in an electron density section through the a-b plane; this peak corresponds to the parameters u = 0.12 and v = 0.43 which are in agreement with the parameters predicted by the optimum arrangement for packing.

Data obtained from the powder diffraction pattern of NaO_2-III at -100° C are tabulated in Table II; observed and calculated intensities are compared in Table III.

Intensities of the lines present in the diffraction pattern of NaO_2-III were estimated visually by comparison with a film of standard exposures. Intensities were calculated from the following equation:

$$I = 0.00165 \quad \frac{(1 + \cos^2 2\theta)}{(\sin^2\theta \cos \theta)} \cdot p \cdot |F|^2$$

where F is the calculated structure factor, p the permutation factor,

θ the Bragg angle, and 0.00165 an arbitrary constant to decrease the calculated intensities to a scale comparable with the observed intensities. As in the case of NaO_2-II for the calculation of the structure factors the atomic scattering power of each oxygen was taken to be $\left[f(O^{-2}) + 3\ f(O)\right] / 4$, and values of $f(O)$, $f(O^{-2})$ and $f(Na^{+})$ were taken from Internationale Tabellen.[10]

The crystal of NaO_2-I was rotated about its face diagonal, $[110]$. After the crystal was cooled below the transition temperature at -77° C, two of the face diagonals were distorted from 7.75 A to 8.52 A and 6.88 A; however, the other four were not greatly distorted since they changed from 7.75 A to 7.78 A.

The photographs indicated quite clearly the presence of twins in NaO_2-III whereas the crystals at room temperature were not twinned. In each of four twins the body diagonal, $[111]$, of the orthorhombic unit cell coincided with the axis of rotation. On the zero layer only two sets of reflections were observed, whereas on the first layer four sets of reflections were observed indicating the presence of four twins. In reciprocal space one set of spots on the zero layer was a reflection of the other set of spots. However, on the first layer there were two pairs of spots, and one pair was a reflection of the other pair.

Twinning in NaO_2-III occurs along the 101 (or $10\bar{1}$) plane. There are two pairs of twins, and the relationship between the pairs of twins is that they are rotated 180° about the $[111]$ axis of the orthorhombic cell. The b axis of one pair of twins is nearly perpendicular to the b axis of the other pair. Details of the recipro-

cal lattice are accounted for satisfactorily by these orientations of the twins.

The four twins arose from distortions of face diagonals of the original cubic unit cell. The predominance of these four twins does not rule out the possible presence of other twins arising from additional distortions or orientations. Perhaps the predominance of only four twins is due to the restriction of the crystal by the capillary. A small number of other reflections on the zero layer and several between the rotation layer lines indicated additional twins; however, it was impossible to ascertain the orientation of these latter twins.

The crystal structure of NaO_2-III was determined independently of the structure of marcasite. The parallel between the two structures of FeS_2 and those of NaO_2 is rather interesting; comparisons among the four structures are tabulated in Table IV.

The transition NaO_2-I $\longrightarrow$ (NaO_2-II) $\longrightarrow$ NaO_2-III has a close parallel in the transition found in NaCN, where a NaCl structure at room temperature possesses rotating CN^- groups; at -10° C this form undergoes a transformation to an orthorhombic structure similar to that of NaO_2-III,[12] the only difference being that the cyanide groups are aligned along two directions, but the groups all lie in parallel planes, just as in the orthorhombic form of NaO_2. Similarities between the two low temperature structures are listed in Table V.

Upon varying the temperature of NaO_2 color changes were observed to occur gradually. The color of NaO_2-III is white, and as the temperature is raised a yellow color appears gradually. NaO_2-I has a

yellow color which upon heating darkens to orange, the color becoming more intense with rising temperature. Apparently the color changes are not associated with the transformations.

V. KO_2-I: CRYSTAL STRUCTURE

Lattice constants of the previously investigated KO_2-II (tetragonal room temperature form) are a = 5.71 A and c = 6.76 A.[13] KO_2-II has a distorted NaCl-type structure, the superoxide groups all being aligned parallel to the tetragonal c axis.[13-15]

Some recent specific heat measurements[11] indicate that KO_2 has a low temperature transition at -52° C. In accordance with this observation potassium superoxide was found to have a low temperature form, KO_2-III, but the powder pattern was not successfully indexed because of its complexity.

Potassium superoxide has a high temperature form (Dr. John Margrave first found evidence indicating this fact, and the author constructed a simple high temperature camera to investigate this problem; powder patterns taken with this camera are the basis for the following information). The structure is cubic, apparently similar to that of NaO_2-I, with a = 6.09 A. Table VI contains observed and calculated intensities for KO_2-I, assuming the superoxide groups to be in disordered orientations (see Templeton and Dauben reference 6, position (3) for the oxygen atoms).

This transition is not rapidly reversible since the high temperature form may be easily quenched to room temperature, a mixture of the two forms being obtained. In fact, even with slow cooling the high form is partially retained at room temperature. Upon heating a

sample of KO_2-I, the transformation to KO_2-I did not occur until about 100° C; on the other hand, the reverse transformation for the same sample did not occur until the temperature was lowered to approximately 60° C. At this temperature or at room temperature a mixture of the two forms, as shown by x-ray diffraction patterns, occurred in every case.

Just as there exists a close correspondence between the two polymorphic pairs of sodium superoxide and FeS_2, there is a close correspondence between two polymorphic modifications of CaC_2[16-18] and KO_2-I and II. Polymorphs of KO_2 and CaC_2 are compared in Table VII.

VI. INTERPRETATION OF RESULTS

It is of interest to compare the transformations of NaO_2-II and KO_2-II into the disordered structures. In the case of KO_2-I $\longrightarrow$ KO_2-II the transformation is sluggish, whereas NaO_2-I transforms into NaO_2-II quite readily. The explanation for this difference lies not in the disordered structures, but rather in the ordered structures. On page five reference was made, in connection with the rotation of the superoxide ions, to four possible sets of positions for the oxygen atoms; since the superoxide ions in NaO_2-II are aligned along the four body diagonals, it is reasonable to believe that the set of positions of oxygen atoms in NaO_2-I is the fourth possibility listed on page five, i.e. each pair of oxygen atoms is parallel to one of the four body diagonals. Assuming this configuration to apply in NaO_2-I, the transformation from NaO_2-I to NaO_2-II would merely involve the freezing of superoxide groups

into correct orientations for the pyrite structure. Even if another set of oxygen positions should actually be the correct one, no drastic rearrangement is necessary in going from one form to another. However, upon investigation of the transformation KO_2-I $\longrightarrow$ KO_2-II it was found that a drastic deformation was necessary: $\underline{a}$ = 6.08 A for KO_2-I must change to $\underline{a}$ = 5.71 A and to $\underline{c}$ = 6.76 A in KO_2-II. Thus each unit cell is deformed to such an extent that the sluggishness of the transformation appears logical.

Because of polymorphism in both NaO_2 and KO_2 it is likely that polymorphs of RbO_2 and CsO_2 also exist.

CHAPTER II. CRYSTAL STRUCTURE OF YTTRIUM TRICHLORIDE

I. INTRODUCTION

Trichlorides of lanthanum, cerium, praseodymium, neodymium, samarium, europium, and gadolinium are known to have the same structure as UCl_3,[19] which has a hexagonal unit cell; the space group is $C6_3/m$. The unit cell contains two cations and six anions, and each cation is surrounded by nine anions.

The trichlorides of the rare earth elements after gadolinium have other structures. Trichlorides of dysprosium, holmium, erbium, thulium, ytterbium, and lutecium are isostructural,[20] but the structure type had not been reported prior to the present work. The purpose of the research reported in this chapter was the investigation of this unknown crystal structure. Since yttrium trichloride has the same structure as these rare earth trichlorides and since it was easily obtainable, it was the most suitable compound for a crystal structure analysis. Terbium trichloride has still another structure which has not yet been determined. $DyCl_3$ is dimorphic[20] with one structure like $TbCl_3$ and the other like YCl_3.

II. EXPERIMENTAL PROCEDURE

A. Preparation of Yttrium Trichloride

Samples of yttrium trichloride were prepared by Charles W. Koch and the author by passing dry hydrogen chloride gas over a few milligrams of pure Y_2O_3 in a platinum boat; for each preparation at approximately 550° C hydrogen chloride was in contact with the sample of Y_2O_3 for at least six hours or more to insure completion of the reaction. The YCl_3 thus obtained was used both for powder x-ray dif-

fraction patterns and for the preparation of single crystals. In order to crystallize the material it was necessary to heat it to 690° C (the melting point of YCl_3 is approximately 680° C). After the fused salt was obtained, a crystalline mass of yttrium trichloride was prepared by cooling the melt over a period of one to two hours. Since yttrium trichloride is extremely deliquescent, the platinum boat still inside the original quartz tube was quickly transferred to a dry box. Inside the dry box, having an atmosphere of argon dried by molten sodium, the mass was broken into tiny crystalline fragments. These tiny anhedral pieces of crystalline yttrium trichloride were transferred to glass capillaries; after the capillaries were sealed, the crystals were ready to be photographed. However, many of the fragments were not satisfactory specimens because they were polycrystalline, and the vast majority of single crystals were in the form of thin plates since the crystalline matter showed marked cleavage properties. Diffraction patterns of crystalline plates afforded inferior data due to absorption errors introduced by the shape of the crystal; this problem was one of the most serious in the entire analysis of the structure.

After a series of equi-inclination Weissenberg photographs had been exposed, the various "reflections" were indexed; as an aid to indexing the patterns reciprocal lattices of the various levels were constructed.

B. Unit Cell

Yttrium trichloride has a monoclinic unit cell: $\underline{a} = 6.92 \pm 0.02$ A, $\underline{b} = 11.94 \pm 0.04$ A, $\underline{c} = 6.44 \pm 0.02$ A, and $\underline{\beta} = 110°20' \pm 30'$.

Since diffraction arose only from $hk\ell$ planes having $h + k = 2n$, with no additional systematic extinctions, the unit cell was C-centered, and the only possible space groups were C2/m, Cm, and C2.[10]

Since the density of yttrium trichloride had been determined by flotation of a crystal of yttrium trichloride in a mixture of two organic liquids, n-butyl phthalate, density = 1.046 gms/cm^3, and bromoform, density = 2.89 gms/cm^3, it was possible to calculate the number of yttrium and chlorine atoms per unit cell. The observed density of yttrium trichloride was 2.55 gms/cm^3 compared to a calculated x-ray density of 2.60 gms/cm^3, assuming four yttrium and twelve chlorine atoms in each unit cell.

III. TRIAL STRUCTURE

Trial arrangements of yttrium atoms may be proposed by using the following information: (1) the lattice constants, (2) the symmetry of each of the three space groups listed above, (3) the fact that there are four yttrium atoms per unit cell, and (4) the assumption that the yttrium-yttrium atomic distances will be a maximum. Upon following this procedure strictly only two arrangements of yttrium atoms are permissible, one with two yttrium atoms in the a-c face, and the other with four yttrium atoms in the a-b face, as shown in Figure 1. The former will be referred to as the "alternate trial structure" while the latter will be the "trial structure".

Since the set of planes 060 diffract x-rays intensely, probably a large fraction of the atoms of the structure lie approximately in planes occurring at intervals of two angstroms (one-sixth of

the b axis) along the b axis and parallel to the a-c face. The relative intensity of 060 to 020 would indicate that the trial structure of four yttrium atoms in the a-b face is more probable than that of the alternate trial structure in which two yttrium atoms occur in the a-c face. In agreement with observation, the trial structure arrangement of yttrium atoms indicates that 060 indeed would give rise to intense diffraction, and according to this arrangement it is logical to assume that two chlorines could be packed into each of the six layers perpendicular to the b axis.

Assuming the closest approach of a chlorine ion to an yttrium ion to be the sum of the ionic radii, the trial arrangements may be visualized by considering spheres with centers located at centers of all yttrium atoms and with radii equal to 2.74 A, the sum of the ionic radius of Y^{+3}, 0.93 A, and of Cl^{-}, 1.81 A. These spheres then leave an open volume which is available for the centers of twelve chlorine atoms. In order to find the actual centers of chlorine atoms in any of the six layers it is necessary first to draw the intersection of the given layer with the spheres mentioned above. This construction, then, gives rise to an area in which it is possible to place centers of chlorine atoms; furthermore this area is limited by the fact that no two chlorine ions may be placed closer together than the ionic diameter of chlorine, i.e. two ionic radii of Cl^{-}.

As an example of the above procedure, consider the packing of chlorine ions into the a-c face of the alternate trial structure, as shown in Figure 2. In this drawing the largest arc represents the

intersection of the "sphere of closest approach" with the a-c face; the three intermediate areas enclosed within the corresponding arcs represent areas within the sphere of closest approach of the corner yttrium atoms. The two smaller areas are not allowed because of the overlap of spheres in neighboring unit cells; the dotted lines represent the closest allowable approach of two chlorine ions. Thus the only areas allowable for centers of chlorine atoms are the two small areas in which tiny circles have been drawn. Logically the optimum arrangement of chlorine ions is for each chlorine ion to touch two yttrium ions; this condition exists only at the intersection of two arcs, as for instance the pair of points indicated by the small circles in Figure 2. Thus in the alternate trial structure these two points were chosen for centers of the two chlorine ions in the a-c face; after this choice was made the appropriate area for chlorine ion centers may be constructed in the plane parallel to the a-c face and two angstroms further along the b axis. Exactly the same procedure is followed here as in the a-c face, with the additional arcs caused by chlorine spheres of closest approach included. Figure 3 shows the result of this construction; since the cross-hatched area is the only possible area in which centers of chlorine ions can occur, it is obvious that two chlorine atoms cannot be packed in the second layer of the alternate trial structure; hence, through strict reasoning based upon assumptions previously made, this alternate trial structure may be eliminated from further consideration. In addition a future argument involving the cleavage of yttrium trichloride parallel to the a-b face indicates this trial

structure is wrong because if any cleavage were present, it would be parallel to the a-c plane.

Thus without further argument our consideration will be focused entirely on the trial structure involving the packing of four yttrium atoms in the a-b face. Upon construction of the allowable area for chlorine ion centers by using the principles already outlined, most probable positions of chlorine atoms in the first layer are indicated by the small circles in Figure 4; Figure 5 shows the most probable positions for the centers of chlorine atoms in the two cross-hatched areas which are the only possible areas for chlorine ion centers to occur in the second layer. By means of successive constructions the entire trial structure was built, and the results are shown in Figures 6, 7, 8, 9, 10, and 11. Figures 12 and 13 are photographs of a model of the trial structure of yttrium trichloride.

The proposed trial structure belongs to the space group C2/m, which is the only centrosymmetric space group[10] of the three original possibilities, C2/m, Cm, and C2. From the positions of atoms in the proposed trial structure, structure factors were calculated for all diffracting planes. The agreement with observed structure factors was rather remarkable for a trial structure; hence proper signs for the structure factors were directly obtainable for electron density calculations for both cross sections and various lines through the unit cell.

IV. ANALYSIS OF STRUCTURE

The origin of the structure was chosen in accordance with Internationale Tabellen[10] to be the lower left hand corner of the sixth

layer of the trial structure as shown in Figure 11. The yttrium and chlorine atoms have the following special positions in the space group C2/m:

yttrium atoms at 4(g): $0y0$; $0\bar{y}0$; $1/2, 1/2 + y, 0$;
$1/2, 1/2 - y, 0$.

chlorine atoms at 4(i): $x0z$, $\bar{x}0\bar{z}$; $1/2 + x, 1/2, z$;
$1/2 - x, 1/2, \bar{z}$.

chlorine atoms at 8(j): xyz; $x\bar{y}z$; $\bar{x}\bar{y}\bar{z}$; $\overline{xyz}$;
$1/2 + x, 1/2 + y, z$; $1/2 + x, 1/2 - y, z$;
$1/2 - x, 1/2 + y, \bar{z}$; $1/2 - x, 1/2 - y, \bar{z}$.

In order to find values for the six parameters occurring in the positions of yttrium and chlorine atoms, the following electron density sections were calculated:

(1) ρ (xoz), for which maxima occured at $x = 0.217$ and $z = 0.242$.

(2) ρ $(x, 0.178, z)$ for which $x = 0.758$ and $z = 0.236$.

Electron densities were also calculated along various lines through the unit cell with the following results:

(1) ρ $(0y0)$, for which $y = 0.166$

(2) ρ $(x, 0, 0.246)$, for which $x = 0.214$

(3) ρ $(0.211, 0, z)$, for which $z = 0.246$

(4) ρ $(0.210, y, 0.246)$, for which $y = 0.178$

(5) ρ $(0.758, 0.176, z)$, for which $z = 0.239$

(6) ρ $(x, 0.176, 0.239)$, for which $x = 0.762$.

From these calculations the following parameters were chosen:

Y 4(g): $y = 0.166 \pm 0.002$

Cl 4(i): $x = 0.214 \pm 0.005$ $z = 0.246 \pm 0.005$

Cl 8(j): $x = 0.238 \pm 0.005$ $y = 0.178 \pm 0.005$ $z = 0.761 \pm 0.005$

Intensity measurements were made by visual comparison of the spots appearing on the Weissenberg photographs with a set of standard intensities obtained from the same crystal of yttrium trichloride. A two-film technique was used in order to estimate more accurately the intensities of overexposed spots;[21] an intensity factor between the films of 3.7 was used.

Structure factors were calculated by using the following equation:

$$F = f_{Y^{+3}} \cos 2\pi (0.166\, k) + f_{Cl^-} \Big[\cos 2\pi (0.214\, h + 0.246\, \ell) + \cos 2\pi (0.762\, h + 0.178\, k + 0.239\, \ell) + \cos 2\pi (0.762\, h - 0.178\, k + 0.239\, \ell) \Big]$$

where $f_{Y^{+3}}$ is the scattering power of the yttrium ion and f_{Cl^-} is that of the chloride ion; h, k, and ℓ are the indices of the particular set of planes for which the calculation of F is made.

Relative structure factors, F, were calculated from observed intensities from the following equation:

$$|F|^2 = a^2 I \frac{(1 + \cos^2 2\theta)}{\sin^2 \theta} \cdot V(\theta)$$

where I is the observed intensity and θ the Bragg angle; $V(\theta)$ is the velocity factor as defined by Tunell.[22] A comparison between calculated and observed structure factors appears in Table VIII. The factor "a" was an arbitrary constant inserted to adjust the observed structure factors to the scale of the calculated structure factors. However, it was observed that the intensities of the layers, $0k\ell$,

$1k\ell$, $2k\ell$, and $3k\ell$ were successively weaker, and hence required increasingly larger values of a. Thus for the zero layer a = 1.055, for the first layer a = 1.25, for the second layer a = 1.50, and for the third layer a = 1.84; these values of a were used in order to obtain minimum discrepancy between observed and calculated structure factors. This use of four values of the arbitrary constant "a" for the four layers concerned is justified by the fact that the glass capillary containing the crystal was quite thick and hence absorbed x-rays highly; in fact, measurements have indicated the intensity of the diffracted x-rays is reduced by a factor of about ten by the glass capillary. Since the equi-inclination Weissenberg method was used, for non-zero layers the x-rays traveled through a greater amount of glass than for the zero layer. Since in general the capillary is inclined to the x-ray beam in the zero layer, each diffracted beam passes through a different thickness of glass; this so complicates the exact calculation of "a" that it is not worthwhile. Because approximate calculations produce average values of "a", such as 1.6 to 1.7 for the third layer compared to 1.8 actually used, it is justifiable to use the constants which produce the minimum discrepancies possible between calculated and observed structure factors.

Essentially diffraction occurs from the outermost shell of the crystal due to the moderately high absorption coefficient of yttrium trichloride. Thus the absorption of the anhedral crystal itself causes sizeable differences in the intensities of diffracted rays from various sets of planes.

Upon application of the formula

$$R = \frac{\Sigma \left| |F|_{obs.} - |F|_{calc.} \right|}{\Sigma |F|_{obs.}}$$

the reliability factor, R, for all diffracting planes hkℓ was 0.21. When only one value of the arbitrary constant, a, was chosen for all hkℓ a reliability factor of 0.25 was obtained.

V. DISCUSSION OF STRUCTURE

The crystal structure of yttrium trifluoride bears no close relationship[23] to that of yttrium trichloride. The unit cell of yttrium trifluoride is orthorhombic with a = 6.36 A, b = 6.86 A, c = 4.39 A, having the space group D_{2h}^{16}-Pnma. There are four yttrium atoms per unit cell, each having nine fluorine neighbors, thus requiring each fluorine to have three yttrium neighbors. This same coordination is found in uranium trichloride. In yttrium trichloride each cation is surrounded by six chlorine atoms in an octahedron; hence each chlorine atom is in contact with only two yttrium atoms. At the present time the crystal structure of yttrium tribromide is unknown, but crystals of yttrium tribromide known to cleave readily, indicating the possibility of a layer structure, perhaps isomorphous with yttrium trichloride. The structure of yttrium tri-iodide is unknown.

The cleavage in yttrium trichloride occurs between two successive layers of anions parallel to the a-b face of the crystal, i.e. the cleavage plane is 001. Serious trouble due to cleavage was encountered in obtaining a crystal suitable for x-ray diffraction patterns; apparently the crystals cleave with such ease that the application of only a slight force is sufficient to overcome the

cohesive forces between layers parallel to the a-b face.

As the parameters previously listed indicate, the structure of yttrium trichloride differs only in minor points from the trial structure; perhaps the most noticeable difference is in the y parameters for yttrium atoms and the 8(j) chlorine atoms. In the trial structure these parameters were necessarily identical because the structure was built by the successive superposition of planes of atoms; thus the 8(j) chlorine atoms and the 4(g) yttrium atoms lay in the same layers of the trial structure. However, in the final structure the 8(j) chlorine atoms do not lie in the same plane as the yttrium atoms. No yttrium atoms lie in planes perpendicular to the $\underline{b}$ axis which contain 4(i) chlorine atoms.

A major point of interest in the structure of yttrium trichloride is the approximate cubic close packing of the chlorine atoms; each chlorine atom is surrounded by twelve other chlorines, giving the distorted cubic-close-packing arrangement. Perhaps this relationship may be visualized most clearly by outlining the distances between the atoms in yttrium trichloride. For instance each yttrium atom has three yttrium neighbors, one at a distance $2 \cdot 0.167 \cdot 11.94 \equiv 2 \cdot y \cdot \underline{b} = 3.99$ A, and two at the distance $\sqrt{(1/2 \cdot 6.92)^2 + (1/2 \cdot 11.94 - 2 \cdot 0.167 \cdot 11.94)^2} = \sqrt{(\underline{a}/2)^2 + (1/2\,\underline{b} - 2\,y\,\underline{b})^2} = 3.98$ A. Although from the parameters and the unit cell dimensions one may calculate in a similar manner all the atomic distances necessary for a complete description of the structure, such calculations are quite cumbersome, and a much more rapid, but slightly less accurate, method was used. From scale

drawings the distances were found quite readily, and the following interatomic distances were obtained in this manner:

Chlorine-chlorine distances in layers parallel to the a-b face of the crystal:

i-Cl
- 2 j-chlorine ions at 3.87 A
- 2 j-chlorine ions at 4.30 A
- 2 j-chlorine ions at 3.83 A

j-Cl
- i-chlorine ion at 3.87 A
- i-chlorine ion at 4.30 A
- i-chlorine ion at 3.83 A
- j-chlorine ion at 3.85 A
- j-chlorine ion at 4.04 A
- j-chlorine ion at 3.83 A

Chlorine-chlorine distances across the cleavage plane:

i-Cl
- 2 j-chlorine ions at 3.90 A
- i-chlorine ion at 4.16 A

j-Cl
- j-chlorine ion at 3.74 A
- i-chlorine ion at 3.90 A
- j-chlorine ion at 3.66 A

Chlorine-chlorine distances across a layer of yttrium ions:

i-Cl
- 2 j-chlorine ions at 3.92 A
- i-chlorine ion at 3.54 A

j-Cl
- j-chlorine ion at 3.69 A
- i-chlorine ion at 3.92 A
- j-chlorine ion at 3.95 A

Yttrium-yttrium distances:

Y
- 2 yttrium ions at 3.99 A
- 1 yttrium ion at 3.98 A

Yttrium-chlorine distances:

Y
- i-chlorine ion at 2.65 A
- i-chlorine ion at 2.72 A

$$Y \begin{cases} 2 \text{ j-chlorine ions at } 2.68 \text{ A} \\ 2 \text{ j-chlorine ions at } 2.80 \text{ A} \end{cases}$$

If the chlorine ions in yttrium trichloride were packed perfectly in a face-centered cubic array, then all chlorine-chlorine interatomic distances would be equal. Since the chlorine-chlorine distances are unequal, the structure of yttrium trichloride consists of a distorted arrangement of closely packed chlorine ions. The structure of yttrium trichloride is a distorted sodium chloride structure with two-thirds of the cations omitted. In this respect other compounds such as cadmium iodide,[24] which has a sodium chloride structure having half the cations omitted, are analogous to yttrium trichloride.

The crystal structure of yttrium trichloride was worked independently of that of aluminum chloride.[25] The two structures are similar, except that the relative magnitudes of a and c are reversed.

$AlCl_3$: C2/m	YCl_3: C2/m
a = 5.92 A	a = 6.92 A
b = 10.22 A	b = 11.94 A
c = 6.16 A	c = 6.44 A
β = 108°	β = 110°20'

$AlCl_3$	x	y	z
Cl 4(i)	0.226	0	0.219
Cl 8(j)	0.250	0.175	0.781
Al 4(g)	0	0.167	0

YCl_3	x	y	z
Cl 4(i)	0.214	0	0.246
Cl 8(j)	0.238	0.178	0.761
Y 4(g)	0	0.166	0

VI. ISOSTRUCTURAL RARE EARTH TRICHLORIDES

Samples of dysprosium, holmium, erbium, thulium, ytterbium and lutecium trichlorides were prepared by Charles W. Koch in a manner similar to that of yttrium trichloride. A comparison of the x-ray powder diffraction patterns indicates the compounds have nearly identical structures since the positions and intensities of the lines are nearly the same in every case. After the pattern of yttrium trichloride was indexed, it was possible to index all the other trichloride powder patterns. In Table IX are listed the various calculated intensities for the powder pattern of yttrium trichloride; observed and calculated $\sin^2\theta$ values for $DyCl_3$, $HoCl_3$, $ErCl_3$, $TmCl_3$, $YbCl_3$ and $LuCl_3$ appear in Table X. Table XI contains corresponding lattice constants for the various isostructural compounds.

An examination of Table XI shows that dysprosium, holmium, erbium, and thulium trichlorides have lattice constants which decrease almost linearly with increasing atomic numbers. This decrease in the volume of the unit cell is in accordance with the well-known lanthanide contraction, in which the ionic or atomic radii of rare earth elements decrease with increasing atomic numbers.

There is a somewhat remarkable change in the structure of ytterbium and lutecium trichlorides, for both the a and c axes have expanded compared with $ErCl_3$ and $TmCl_3$; however, the b axis has continued to shrink as expected. The total volume of the unit cell increases correspondingly, but the lattice constants of lutecium trichloride are smaller than those of ytterbium trichloride, just as one would predict. Qualitatively speaking, this abrupt change in the structure is probably due to the crowding of the atoms caused by

contractions of the unit cell as shown in Table XI. The change may be visualized as a compression along the b axis. If the force were great enough, one would expect both the a and c axes to increase, just as in $YbCl_3$ and $LuCl_3$. The various forces involved are complicated, and since exact coordinates of the atoms are not known in any case but YCl_3, it is impossible to calculate accurate interatomic distances; thus at present a quantitative understanding of this structural anomaly would be most difficult to obtain.

Theoretically in the $AlCl_3$ and YCl_3 type structure the axial ratio b/a should be equal to the square root of three in order for the cations to be surrounded by three cationic neighbors all at equal distances; by referring to Table XI this rule is seen to hold quite rigidly for $AlCl_3$, YCl_3, $DyCl_3$, $HoCl_3$, $ErCl_3$, and $TmCl_3$. However, for $YbCl_3$ and $LuCl_3$ the ratio has altered somewhat, indicating the change in the structure. Thus it would be interesting to know the coordinates of the various atoms in the latter two structures in order to understand better the reason for the change in the structure.

Structures of the trichlorides of gallium, indium, and thallium are unknown; $ScCl_3$ has a rhombohedral AsI_3 structure,[26] and $AcCl_3$ is isostructural with UCl_3.[19] At the present time further investigations are being carried out on $GaCl_3$, $InCl_3$, and $TlCl_3$ in an attempt to find whether these chlorides possibly have one of the various trichloride structures now known.

VII. ACKNOWLEDGMENT

These investigations were originally suggested by Dr. David H. Templeton, to whom I am greatly indebted for the helpful assistance and guidance offered throughout this research. In addition the writer wishes to express his appreciation for the assistance provided by his colleagues Mrs. Carol H. Dauben, Mrs. Helena W. Ruben, Dr. Allan Zalkin, and Mr. Edward S. Clark. Dr. John Margrave discovered the high temperature transition of potassium superoxide, and Dr. S. S. Todd determined specific heat measurements of both sodium and potassium superoxides.

This work was performed under the auspices of the U. S. Atomic Energy Commission.

VIII. REFERENCES

1. A. V. Harcourt, J. Chem. Soc., 14, 267 (1862).
2. W. Holt and W. E. Sims, J. Chem. Soc., 65, 432 (1894).
3. E. Rengade, Ann. Chim. Phys., (8), 11, 348 (1907).
4. W. H. Schecter, J. K. Thompson and J. Kleinberg, J. Am. Chem. Soc., 71, 1816 (1949).
5. S. E. Stephanou, W. H. Schechter, W. J. Argersinger, and J. Kleinberg, J. Am. Chem. Soc., 71, 1819 (1949).
6. D. H. Templeton and C. H. Dauben, J. Am. Chem. Soc., 72, 2251 (1950).
7. H. M. Parker and W. J. Whitehouse, Philos. Mag., 14, 939 (1932).
8. M. J. Buerger, J. Am. Min., 16, 361 (1931).
9. M. J. Buerger, Z. Kristalogr., (A), 97, 504 (1937).
10. Internationale Tabellen zur Bestimmung von Kristallstrukturen, Vol. I and II, Borntraeger, Berlin (1935).
11. S. S. Todd, unpublished work (1952).
12. H. J. Verweel and J. M. Bijvoet, Z. Kristallogr., (A), 100, 201 (1938).
13. W. Kassatoschkin and W. Kotow, J. Chem. Phys., 4, 458 (1936).
14. A. Helms, Z. angew. Chem., 51, 498 (1938).
15. A. Helms and W. Klemm, Z. anorg. allgem. Chem., 241, 97 (1939).
16. M. A. Bredig, J. of Phys. Chem., 46, 801 (1942).
17. H. H. Franck, M. A. Bredig and G. Hoffmann, Z. anorg. Chem., 232, 61 (1937).
18. H. H. Franck, M. A. Bredig and Kin-Hsing Kou, Z. anorg. allgem. Chem., 232, 75 (1937).

19. W. H. Zachariasen, US AEC Report AECD-2091 (1944-1946).

20. E. Hohmann and H. Bommer, Z. fur anorg u. allgem. Chemie, 248, 373 (1941).

21. J. J. De Lange, J. M. Robertson, and I. Woodward, Proc. Roy. Soc. (London), A171, 398 (1939).

22. G. Tunell, Am. Min., 24, 448 (1939).

23. A. Zalkin, Dissertation, Univ. of Calif. (1951).

24. G. Hägg, R. Kiessling and E. Linden, Arkiv. Kemi. Min. Geol., 16B, No. 4 (1942).

25. J. A. A. Ketelaar, C. H. MacGillavry and P. A. Renes, Rec. trav. chim., 66, 501 (1947).

26. L. Vegard, Skrifter Norske Videnskaps--Akad. Oslo. I. Mat.--Naturv. Klasse, No. 2 (1947).

TABLE I

Calculated and Observed Intensities of NaO_2-II

Cu Kα Radiation: λ = 1.5418 A

hkℓ	$\sin^2\theta$ (obs.)	d in A	Observed Intensities	Calculated Intensities[6]
100			0	0
110			0	0
111			0	0.02
200	0.0797	2.72	43	53
210	0.0986	2.45	3.4	4.5
211	0.1187	2.24	4.3	5.0
220	0.1590	1.93	25	22
300, 221	0.1773	1.83	1.3	1.1
310			0	0
311	0.2182	1.64	7	7.8
222	0.2380	1.58	5	5.1
320	0.2591	1.51	3.4	3.3
321	0.2777	1.46	4.3	4.4
400	0.3176	1.37	1.3	0.7
410	0.3372	1.32	1.7	1.8
411, 330	0.3555	1.29	0.9	0.8
331	0.3757	1.26	4.3	3.4
420	0.3960	1.22	3.4	2.4
421			0	0.3
332			0	0.1
422	0.4738	1.12	3.4	1.9
500, 430	0.4965	1.09	1.3	1.2
510, 431	0.5140	1.07	1.7	1.8
511, 333	0.5331	1.05	4.3	5.7

TABLE II

Diffraction Data for NaO_2-III
Cu Kα Radiation: λ = 1.5418 A

hkℓ	Intensity	$Sin^2\theta$	d in A
020	vs	0.0774	2.76
101	vvs	0.0821	2.68
111	vw	0.1023	2.40
120	m	0.1087	2.34
200	m	0.1308	2.13
210	w	0.1514	1.98
121	s	0.1603	1.92
002, 211	vvs	0.200	1.72
220, 130	ms	0.2089	1.68
031	m	0.2248	1.62
221, 131	m	0.2576	1.52
022	s	0.2793	1.46
122, 040, 310	s	0.3127	1.38
202	m	0.3339	1.33
231	mw	0.3555	1.29
320	w	0.3706	1.26
141	vw	0.3943	1.23
132, 222	m	0.4097	1.20
241	w	0.4930	1.10
312, 232	m	0.5105	1.08
331	w	0.5209	1.07
142	w	0.5401	1.05
411	w	0.5885	1.00

TABLE III

Calculated and Observed Intensities of NaO_2-III

$hk\ell$	$I_{obs.}$	$I_{calc.}$	$hk\ell$	$I_{obs.}$	$I_{calc.}$
110	<2	0.5	321	<2	1.9
101	160	160	312	4	0.7
011	<2	2.3	232		1.0
111	6	10.4	132	6	3.5
200	12	11.9	222		5.1
020	80	67.5	231	4	6.1
002	20	22.1	123	<2	5.1
211		21.1	213	<2	2.0
210	<2	5.4	322	<2	1.2
120	16	15.4	223	<2	1.8
121	48	60.7	330	<2	1.4
112	<2	0.9	303	<2	0.13
220	20	9.1	033	<2	1.1
130		7.6	331	3	2.5
			400		0
202	3	3.8	313		0
022	8	12.5	133	<2	0.11
221	8	11.2			
131		0.6	004	<2	2.6
212	<2	1.8			
122	8	3.1	140	<2	1.4
040		0.5	411	2	8.3
310		10.2	141	2	2.1
301	<2	1.9	114	<2	0.2

TABLE III (continued)

hkℓ	$I_{obs.}$	$I_{calc.}$	hkℓ	$I_{obs.}$	$I_{calc.}$
031	4	7.3	420	<2	0.2
103	<2	5.3	402	<2	0
013	<2	0	240	<2	1.6
311	<2	0.9	042	<2	0.4
113	<2	0.4	024	<2	3.4
320	2	1.3	204	<2	2.1
230	<2	0	421	<2	0.2
412	<2	0			
142, 410	3	1.1, 0			
241	3	0.3			

TABLE IV

Comparisons Among Pyrite, Marcasite, and NaO_2 Low Temperature Structures

Space Group: T_h^6--Pa3		D_{2h}^{12}--Pnnm	
Pyrite	NaO_2-II	Marcasite	NaO_2-III
a 5.405 A	5.48 A	4.436 A	4.26 A
b 5.405 A	5.48 A	5.414 A	5.54 A
c 5.405 A	5.48 A	3.381 A	3.44 A
V 157.9 A^3	164.6 A^3	81.2 A^3	81.2 A^3
MV 39.5 A^3	41.1 A^3	40.6 A^3	40.6 A^3
u 0.386	0.439	0.200	0.12
v --	--	0.378	-0.42
R--X 2.26 A	2.42 A	2.25 and 2.23 A	2.33 A
X--X 2.14 A	1.35 A	2.21 A	1.35 A

a, b, and c are unit cell dimensions.

V is the volume of the unit cell.

MV is the volume of one molecule.

u and v are parameters in the respective structures.

R--X is the distance between centers of metal and oxygen or sulfur atoms.

X--X is the distance between centers of oxygen (sulfur) atoms in O_2^- (S_2) groups.

TABLE V

Comparisons Among NaCN-I and II
and NaO_2-I and III

NaCn-I	NaO_2-I	NaCn-II	NaO_2-III
a 5.87 A	5.49 A	4.71 A	4.26 A
b 5.87 A	5.49 A	5.61 A	5.54 A
c 5.87 A	5.49 A	3.74 A	3.44 A
V 203 A^3	165.5 A^3	98.8 A^3	81.2 A^3
MV 50.8 A^3	41.4 A^3	49.4 A^3	40.6 A^3
X--Y 1.06 A	1.35 A	1.06 A	1.35 A

a, b, and c are unit cell dimensions.

V is the volume of the unit cell.

MV is the volume of one molecule.

X--Y is the distance between centers of oxygen (carbon and nitrogen) atoms in O_2^- (CN^-) groups.

TABLE VI

Diffraction Data for KO_2-I
Cu Kα Radiation: λ = 1.5418 A

hkℓ	$I_{obs.}$	$I_{calc.}$	$\sin^2\theta_{obs.}$	d in A
111	5.4	4.9	0.0483	3.50
200	41	41.0	0.0640	3.04
220	14	17.3	0.1278	2.16
311	4.5	5.8	0.1759	1.83
222	4.5	4.8	0.1915	1.76
400	---	1.3	---	---
331	3.2	3.2	0.3038	1.40
420	3.2	3.1	0.3200	1.36
422	---	2.3	---	---
333	---	0.6	---	---
511		2.8		
440	---	0.8	---	---

TABLE VII

Comparisons of Polymorphs of KO_2 and CaC_2

KO_2-I	$\xrightarrow[\text{Sluggish}]{\approx 80^\circ C}$	KO_2-II	$\xrightarrow[\text{Rapid}]{-52^\circ C}$	KO_2-III
Face-centered		Tetragonal:		Structure
Cubic: NaO_2-I		CaC_2 Structure		Unknown
Structure				

CaC_2-IV	$\xrightarrow[\text{Rapid}]{450^\circ C}$	CaC_2-III	$\xrightarrow[\text{Sluggish}]{(450^\circ C-25^\circ C)}$	CaC_2-I	$\longrightarrow$
Face-centered		(Metastable)		Tetragonal	
Cubic lattice		Structure			
		Unknown			

$$\cdots \xrightarrow[\text{Rapid}]{25^\circ C} CaC_2\text{-II}$$

Structure

Unknown

TABLE VIII

Calculated and Observed Structure Factors of YCl_3

hkℓ	Calculated F	Observed F	hkℓ	Calculated F	Observed F
001	+37.1	37.1	062	-2.3	0
002	-8.7	10.3	063	+18.0	17
003	+21.1	21.2	064	+41.9	34
004	+47.5	43.5	065	+24.7	15.4
005	+26.9	22.3	080	-17.1	19.1
006	-8.9	0	081	-11.9	11.7
007	+9	0	082	-5.3	0
020	-20.3	30.8	083	-8.3	0
021	-17.1	19.1	084	-14.0	12.7
022	-12.1	12.7	0,10,0	-1.4	0
023	-11.6	13.8	0,10,1	-9.5	13.8
024	-12.6	13.8	0,10,2	-18.0	18
025	-11.7	11.1	0,10,3	-9.9	0
026	-8	0	0,12,0	+36.5	24.4
040	-9.5	9.6	0,12,1	+19.2	15.9
041	-14.4	19.1	0,12,2	-1	0
042	-21.1	22.3	110	20.6	25
043	-12	11.1	111	+14.8	17.4
044	-8.2	0	$11\bar{1}$	+18.3	20.9
045	-9.6	11.7	112	+11.4	13.8
060	+55.8	71.1	$11\bar{2}$	+10.8	8.6
061	+27.9	31.8	113	+14.3	17.7

TABLE VIII (continued)

$hk\ell$	Calculated F	Observed F	$hk\ell$	Calculated F	Observed F
$11\bar{3}$	+12	10.3	151	+18.4	22.3
114	+12.4	0	$15\bar{1}$	+8.7	10
$11\bar{4}$	+15.1	11.8	152	+10.2	11.6
115	+9.2	0	$15\bar{2}$	+8.5	11.2
$11\bar{5}$	+11.6	0	153	+6.9	0
116	+8	0	$15\bar{3}$	+15.4	17.3
$11\bar{6}$	+6.4	0	154	+10.6	0
$11\bar{7}$	+8.3	0	$15\bar{4}$	+15.5	12.8
130	-30.1	41.7	155	+12.7	0
131	-65.3	69.4	$15\bar{5}$	+12.1	0
$13\bar{1}$	-8.9	11.9	156	+9	0
132	-31.0	37.8	$15\bar{6}$	+4.2	0
$13\bar{2}$	-25.1	29.6	170	+14.1	15.2
133	+2	0	171	+5.2	0
$13\bar{3}$	-54.4	48.7	$17\bar{1}$	+19.2	31.7
134	-15	15.5	172	-8.4	12.4
$13\bar{4}$	-18.8	22.2	$17\bar{2}$	+9.8	11.6
135	-39.3	34	173	+16.0	16.1
$13\bar{5}$	-1.9	0	$17\bar{3}$	+4.4	0
136	-24.9	12.9	174	+11.3	0
$13\bar{6}$	-11.9	13.6	$17\bar{4}$	+10.7	0
$13\bar{7}$	-35.4	12.7	175	+4.1	0
150	+17.4	24.2	$17\bar{5}$	+11.7	0

TABLE VIII (continued)

hkℓ	Calculated F	Observed F	hkℓ	Calculated F	Observed F
$17\bar{6}$	+8.0	0	201	+24.8	29.8
190	-20.6	20.2	$20\bar{1}$	+28.8	does not appear on film
191	-42.3	45.5	202	+54.2	63.2
$19\bar{1}$	-0.9	0	$20\bar{2}$	+63.4	57.4
192	-22.9	21.5	203	+28.3	37.7
$19\bar{2}$	-18.6	21	$20\bar{3}$	+30.6	23
193	+1.5	0	204	-1.8	0
$19\bar{3}$	-39.3	30.9	$20\bar{4}$	-0.8	0
194	-11.8	0	205	+7.3	0
$19\bar{4}$	-21.6	12.5	$20\bar{5}$	+14.3	14.4
195	-34.3	17.5	206	+35.7	23.2
$19\bar{5}$	+1.5	0	$20\bar{6}$	+38.2	24.2
$19\bar{6}$	-10	0	$20\bar{7}$	+24.5	0
1,11,0	+12	12.5	220	-11.3	14.9
1,11,1	+15.8	14.7	221	-20	24.7
$1,11,\bar{1}$	+3.3	0	$22\bar{1}$	-6.6	7.7
1,11,2	+9.9	0	222	-18.6	17.7
$1,11,\bar{2}$	+4.9	0	$22\bar{2}$	-16	23
1,11,3	+14.3	0	223	-7.4	0
$1,11,\bar{3}$	+13.8	0	$22\bar{3}$	-20.6	22.2
1,13,0	+9.3	0	224	-6.4	0
$1,13,\bar{1}$	+18.6	11.5	$22\bar{4}$	-10.5	0
200	+7.6	8.6	225	-11.4	0

TABLE VIII (continued)

hkℓ	Calculated F	Observed F	hkℓ	Calculated F	Observed F
$22\bar{5}$	-3.8	0	263	+25.1	24.1
226	-11.0	0	$26\bar{3}$	+23.2	25
$22\bar{6}$	-9.5	0	264	-1.0	0
$22\bar{7}$	-14.6	0	$26\bar{4}$	-0.7	0
$22\bar{8}$	-8.2	0	265	+9.6	0
240	-17.2	26.4	$26\bar{5}$	+18.4	12.7
241	-18.1	22.8	266	+32.6	13.5
$24\bar{1}$	-8.2	11.1	$26\bar{6}$	+35.8	17.1
242	-9.1	0	$26\bar{7}$	+22.7	9.5
$24\bar{2}$	-8.8	9.7	280	-4.6	0
243	-6.3	0	281	-15.5	19.1
$24\bar{3}$	-17	17.8	$28\bar{1}$	-4.6	0
244	-11.8	13.9	282	-16.2	16.4
$24\bar{4}$	-15	16	$28\bar{2}$	-16.4	17
245	-12.0	0	283	-6.3	0
$24\bar{5}$	-5.9	0	$28\bar{3}$	-17.3	15
246	-6.8	0	284	-2.7	0
$24\bar{6}$	-5.7	0	$28\bar{4}$	-5.3	0
260	-1.4	0	$28\bar{5}$	-13.0	0
261	+20.5	25.7	2,10,0	-17.3	18
$26\bar{1}$	+24.3	33.6	2,10,1	-13.9	0
262	+44.6	48.8	2,10,$\bar{1}$	-7.0	0
$26\bar{2}$	+47.9	47.2	2,10,2	-2.1	0

TABLE VIII (continued)

hkℓ	Calculated F	Observed F	hkℓ	Calculated F	Observed F
2,10,$\bar{2}$	-1.7	0	330	-27.5	32.1
2,10,3	-5.2	0	331	-0.9	0
2,10,$\bar{3}$	-6.8	0	33$\bar{1}$	-53.9	58.9
2,10,$\bar{4}$	-16.5	15.6	332	-18	20.5
2,10,$\bar{5}$	-7.3	0	33$\bar{2}$	-24.3	37.8
2,12,0	-0.4	0	333	-41.1	41.6
2,12,$\bar{1}$	+17.4	22.9	33$\bar{3}$	+0.1	0
2,12,2	+33.6	21.5	334	-24.7	24.7
2,12,$\bar{2}$	+34.3	22.1	33$\bar{4}$	-19.2	15.5
2,12,3	+20.5	12.5	335	-1.9	0
310	+4.8	7.7	33$\bar{5}$	-40.2	28.5
311	+21.5	14.8	336	-5.9	0
31$\bar{1}$	+14.3	0	33$\bar{6}$	-23.6	16.4
312	+17.8	19.5	33$\bar{7}$	-1.1	0
31$\bar{2}$	+22.6	24.9	350	+3.4	0
313	+11.8	15.6	351	+5.6	0
31$\bar{3}$	+13	10.4	35$\bar{1}$	+17.4	22.6
314	+4.4	0	352	+17.1	22.6
31$\bar{4}$	+3.6	0	35$\bar{2}$	+21.3	23.7
315	+6.6	0	353	+15.2	18.5
31$\bar{5}$	+9.3	0	35$\bar{3}$	+7.8	0
31$\bar{6}$	+16.4	0	354	+4.5	0
31$\bar{7}$	+10.5	0	35$\bar{4}$	+0.8	0

TABLE VIII (continued)

$hk\ell$	Calculated F	Observed F	$hk\ell$	Calculated F	Observed F
355	+2.2	0	390	-21.1	24.5
$35\bar{5}$	+10.1	16.4	391	-0.2	0
356	+10.9	0	$39\bar{1}$	-38.4	41.7
$35\bar{6}$	+16.0	15.5	392	-13.3	0
$35\bar{7}$	+7.3	0	$39\bar{2}$	-19.9	18.5
370	+4.5	0	393	-34.1	21.9
371	+22.7	17.2	$34\bar{3}$	-14.2	0
$37\bar{1}$	+5.9	0	394	-20.7	23.5
372	+15	16.7	$39\bar{4}$	-14.7	16.4
$37\bar{2}$	+16.1	21.3	$39\bar{5}$	-33.5	18
373	+5.8	0	3,11,0	+1.1	0
$37\bar{3}$	+15.5	21.4	3,11,1	+0.9	0
374	+3.1	0	$3,11,\bar{1}$	+15.0	0
$37\bar{4}$	+5.3	0	3,11,2	+13.5	0
375	+4.3	0	$3,11,\bar{2}$	+16.7	0

TABLE IX

Calculated Powder Pattern
Intensities of Yttrium Trichloride

$hk\ell$	$\sin^2\theta$	I	$hk\ell$	$\sin^2\theta$	I
001	0.0164	166	240	0.1237	4
020	0.0167	38	$15\bar{1}$	0.1238	5
$11\bar{1}$	0.0238	46	310	0.1324	1
021	0.0331	44	$31\bar{2}$	0.1324	13
111	0.0458	20	$11\bar{3}$	0.1335	4
130	0.0517	60	$20\bar{3}$	0.1392	9
$13\bar{1}$	0.0571	6	132	0.1394	23
$11\bar{2}$	0.0623	5	151	0.1458	4
002	0.0658	2	003	0.1480	5.5
040	0.0667	6	$24\bar{2}$	0.1486	4
$22\bar{1}$	0.0682	3	$33\bar{1}$	0.1492	65
220	0.0737	10	060	0.1501	34
131	0.0791	200	$22\bar{3}$	0.1559	9
$20\bar{2}$	0.0819	88	241	0.1620	5
041	0.0831	11	$15\bar{2}$	0.1623	1
201	0.0953	10	023	0.1647	2
$13\bar{2}$	0.0956	27	$33\bar{2}$	0.1657	11
$22\bar{2}$	0.0986	8	330	0.1657	17
112	0.1061	7	061	0.1665	15
221	0.1120	10	202	0.1667	29
$24\bar{1}$	0.1182	1	$13\bar{3}$	0.1668	57
150	0.1184	8	311	0.1817	2

TABLE IX (continued)

$hk\ell$	$\sin^2\theta$	I	$hk\ell$	$\sin^2\theta$	I
$31\bar{3}$	0.1817	4	$26\bar{3}$	0.2893	4
222	0.1834	3	$33\bar{4}$	0.2971	.8
113	0.1993	3	332	0.2973	3
$26\bar{1}$	0.2016	10	063	0.2981	3
$24\bar{3}$	0.2059	5	$24\bar{4}$	0.2990	1
152	0.2061	2	172	0.3062	1
043	0.2147	1	262	0.3168	18
$35\bar{1}$	0.2159	3	370	0.3325	2
170	0.2185	3	$37\bar{2}$	0.3325	3
$17\bar{1}$	0.2239	2	$15\bar{4}$	0.3375	2
$26\bar{2}$	0.2320	31	$28\bar{2}$	0.3487	1
$35\bar{2}$	0.2324	5	190	0.3518	3
$15\bar{3}$	0.2335	2	$19\bar{2}$	0.3518	3
$11\bar{4}$	0.2375	4	$20\bar{5}$	0.3583	1
261	0.2454	4	134	0.3586	2
203	0.2608	5	281	0.3621	1
$17\bar{2}$	0.2624	.5	352	0.3640	1
004	0.2630	12	$11\bar{5}$	0.3746	1
312	0.2640	.6	313	0.3791	1
080	0.2668	1	191	0.3792	14
$13\bar{4}$	0.2708	7	371	0.3818	.5
024	0.2797	1	$37\bar{3}$	0.3818	.5
081	0.2832	2	173	0.3994	.7

TABLE IX (continued)

hkℓ	$\sin^2\theta$	I	hkℓ	$\sin^2\theta$	I
$28\bar{3}$	0.4060	2	206	0.5172	4
263	0.4109	4	135	0.5176	9
005	0.4110	2	1,11,0	0.5186	0.8
$33\bar{5}$	0.4122	10	$31\bar{6}$	0.5268	2
333	0.4124	12	084	0.5298	0.5
064	0.4131	12	$22\bar{6}$	0.5339	0.5
025	0.4277	1.2	1,11,1	0.5460	0.5
282	0.4335	0.8	$33\bar{6}$	0.5601	1
192	0.4395	3	334	0.5603	4
$39\bar{1}$	0.4493	10	065	0.5611	3
372	0.4641	1	$13\bar{6}$	0.5777	1
244	0.4644	1	0,12,0	0.6003	4
390	0.4658	3	$3,11,\bar{1}$	0.6161	0.5
$39\bar{2}$	0.4658	2	$35\bar{6}$	0.6268	2
$19\bar{3}$	0.4669	10	$3,11,\bar{2}$	0.6362	1
2,10,0	0.4739	0.4	$2,10,\bar{4}$	0.6492	0.4
045	0.4777	1.2	$2,12,\bar{1}$	0.6518	2
$35\bar{5}$	0.4789	7	$26\bar{6}$	0.6673	7
353	0.4791	0.6	$2,12,\bar{2}$	0.6822	8
0,10,2	0.4827	0.5	$20\bar{7}$	0.7090	1
$26\bar{5}$	0.5084	1	136	0.7093	4
2,10,1	0.5122	0.8	$39\bar{5}$	0.7123	7

TABLE IX (continued)

$hk\ell$	$\sin^2\theta$	I	$hk\ell$	$\sin^2\theta$	I
393	0.7125	8	007	0.8055	0.3
$1,13,\bar{1}$	0.7241	0.4	195	0.8176	10
$22\bar{7}$	0.7257	2	$26\bar{7}$	0.8591	4
$37\bar{6}$	0.7269	1	$39\bar{6}$	0.8602	3
2,12,2	0.7670	10	2,12,3	0.8611	4
$24\bar{7}$	0.7757	2	$19\bar{6}$	0.8778	2
$13\bar{7}$	0.7804	8	266	0.9305	16
206	0.7804	5	$2,12,\bar{5}$	0.9589	3
$28\bar{6}$	0.7840	0.6			

TABLE X

Observed and Calculated $Sin^2\theta$
for Rare Earth Trichlorides

hkℓ	$DyCl_3$ $Sin^2\theta_{Calc.}$	$DyCl_3$ $Sin^2\theta_{Obs.}$	$DyCl_3$ $I_{Obs.}$	$HoCl_3$ $Sin^2\theta_{Calc.}$	$HoCl_3$ $Sin^2\theta_{Obs.}$	$HoCl_3$ $I_{Obs.}$
020	0.0166	0.0160	s	0.0168	0.0162	s
001	0.0162	0.0160	s	0.0166	0.0162	s
110	0.0184	0.0179	w	0.0186	0.0184	w
$11\bar{1}$	0.0236	0.0230	w	0.0241	0.0238	w
021	0.0328	0.0320	vw	0.0334	0.0332	w
111	0.0456	0.0450	vw	0.0463	0.0456	vw
130	0.0515	0.0502	s	0.0522	0.0518	s
$20\bar{1}$	0.0510	0.0502	s	0.0520	0.0518	s
$13\bar{1}$	0.0567	---		0.0577	---	
$11\bar{2}$	0.0612	---		0.0628	---	
040	0.0664	---		0.0672	---	
$20\bar{2}$	0.0776	0.0780	vs	0.0796	0.0797	s
131	0.0787	0.0780	vs	0.0799	0.0797	s
022	0.0814	---		0.0832	---	
041	0.0826	---		0.0838	---	
$13\bar{2}$	0.0943	0.0949	m	0.0957	0.0960	mw
$22\bar{2}$	0.0942	0.0949	m	0.0964	0.0960	mw
201	0.0950	0.0949	m	0.0964	0.0960	mw
112	0.1052	---		0.1072	---	
221	0.1116	---		0.1132	0.1126	vw
150	0.1180	---		0.1194	0.1175	vw
240	0.1232	---		0.1248	0.1259	vw
$15\bar{1}$	0.1232	---		0.1249	0.1259	vw
$31\bar{2}$	0.1308	0.1312	vw	0.1336	0.1334	vw

TABLE X (continued)

hkl	$DyCl_3$ $Sin^2\theta_{Calc.}$	$DyCl_3$ $Sin^2\theta_{Obs.}$	$DyCl_3$ $I_{Obs.}$	$HoCl_3$ $Sin^2\theta_{Calc.}$	$HoCl_3$ $Sin^2\theta_{Obs.}$	$HoCl_3$ $I_{Obs.}$
042	0.1312	0.1312	vw	0.1336	0.1334	vw
$11\bar{3}$	0.1312	0.1312		0.1347	0.1334	vw
$20\bar{3}$	0.1366	---		0.1404	0.1402	w
132	0.1386	0.1386	w	0.1408	0.1402	w
$24\bar{2}$	0.1440	---		0.1468	---	
151	0.1452	---		0.1471	---	
003	0.1458	---		0.1495	0.1512	s
060	0.1494	0.1482	ms	0.1512	0.1512	s
$33\bar{1}$	0.1483	0.1482	ms	0.1507	0.1512	s
023		---		0.1663	---	
$13\bar{3}$	0.1643	0.1663	ms	0.1684	0.1683	s
330	0.1651	0.1663	ms	0.1674	0.1683	s
061	0.1656	0.1663	ms	0.1678	0.1683	s
202	0.1656	0.1663	ms	0.1684	0.1683	s
$33\bar{2}$	0.1639	0.1663	ms	0.1672	0.1683	s
311	0.1812	---		0.1837	---	
$31\bar{3}$	0.1788	---		0.1833	---	
222	0.1822	---		0.1852	---	
113	0.1972	(0.1997)	vw	0.2013	0.1996	vw
$26\bar{1}$	0.2004	0.1997	vw	0.2032	---	
043	0.2122	0.2141	vw	0.2167	0.2177	vw
400	0.2272	0.2278	w	0.2304	0.2306	vw
$26\bar{2}$	0.2270	0.2278	w	0.2308	0.2306	vw
$24\bar{3}$	0.2030	---		0.2077	---	

TABLE X (continued)

hkℓ	$ErCl_3$ $Sin^2\theta_{Calc.}$	$ErCl_3$ $Sin^2\theta_{Obs.}$	$ErCl_3$ $I_{Obs.}$	$TmCl_3$ $Sin^2\theta_{Calc.}$	$TmCl_3$ $Sin^2\theta_{Obs.}$	$TmCl_3$ $I_{Obs.}$
020	0.0171	0.0164	s	0.0173	0.0168	vs
001	0.0169	0.0164	s	0.0171	0.0168	vs
110	0.0189	0.0188	w	0.0191	0.0191	mw
$11\bar{1}$	0.0247	0.0242	mw	0.0248	0.0248	m
021	0.0340	0.0335	mw	0.0342	0.0342	mw
111	0.0469	0.0460	vw	0.0478	0.0468	w
130	0.0531	0.0527	vw	0.0538	0.0538	s
$20\bar{1}$	0.0532	0.0527	s	0.0537	0.0538	s
131	0.0585	---		0.0595	---	
$11\bar{2}$	0.0647	---		0.0646	0.0636	vw
040	0.0685	0.0694	vw	0.0693	0.0702	vw
$20\bar{2}$	0.0816	0.0808	vs	0.0820	0.0813	vs
131	0.0811	0.0808	vs	0.0824	0.0813	vs
022	0.0851	---		0.0857	---	
041	0.0855	---		0.0860	---	
$13\bar{2}$	0.0985	0.0974	ms	0.0992	0.0985	m
$22\bar{2}$	0.0987	0.0974	ms	0.0993	0.0985	m
201	0.0975	0.0974	ms	0.0997	0.0985	m
112	0.1091	---		0.1106	---	
221	0.1146	0.1142	vw	0.1170	0.1152	w
150	0.1206	0.1202	w	0.1231	0.1226	w
240	0.1269	0.1264	vw	0.1285	0.1289	w
$15\bar{1}$	0.1264	0.1264	vw	0.1287	0.1289	w
$31\bar{2}$	0.1367	0.1354	m	0.1368	0.1368	mw

TABLE X (continued)

hkℓ	$ErCl_3$ $Sin^2\theta_{Calc.}$	$ErCl_3$ $Sin^2\theta_{Obs.}$	$ErCl_3$ $I_{Obs.}$	$TmCl_3$ $Sin^2\theta_{Calc.}$	$TmCl_3$ $Sin^2\theta_{Obs.}$	$TmCl_3$ $I_{Obs.}$
042	0.1361	0.1354	w	0.1377	0.1368	mw
$11\bar{3}$	0.1377	0.1354	w	0.1385	0.1368	mw
$20\bar{3}$	0.1439	0.1419	m	0.1445	0.1430	m
132	0.1424	0.1419	m	0.1452	0.1430	m
$24\bar{2}$	0.1505	---		0.1509	0.1500	vw
151	0.1487	---		0.1517	0.1500	vw
003	0.1521	0.1541	s	0.1539	---	
060	0.1541	0.1541	s	0.1559	0.1560	s
$33\bar{1}$	0.1535	0.1541	s	0.1557	0.1560	s
023	0.1692	0.1700	s	0.1712	0.1710	s
$13\bar{3}$	0.1719	0.1700	s	0.1732	0.1710	s
330	0.1699	0.1700	s	0.1731	0.1710	s
061	0.1710	0.1700	s	0.1730	0.1710	s
202	0.1704	0.1700	s	0.1740	0.1710	s
$33\bar{2}$	0.1713	0.1700	s	0.1725	0.1710	s
311	0.1861	---		0.1888	0.1881	w
$31\bar{3}$	0.1888	---		0.1870	0.1881	w
222	0.1879	---		0.1911	---	
113	0.2043	0.2064	mw	0.2075	0.2092	w
$26\bar{1}$	0.2072	0.2064	mw	0.2096	0.2092	w
$24\bar{3}$	0.2133	---		0.2134	---	
043	0.2206	0.2223	w	0.2232	0.2252	w
400	0.2336	0.2349	m	0.2384	0.2374	ms
$26\bar{2}$	0.2357	0.2349	m	0.2379	0.2374	ms

TABLE X (continued)

hkℓ	$YbCl_3$ $Sin^2\theta_{Calc.}$	$YbCl_3$ $Sin^2\theta_{Obs.}$	$YbCl_3$ $I_{Obs.}$	$LuCl_3$ $Sin^2\theta_{Calc.}$	$LuCl_3$ $Sin^2\theta_{Obs.}$	$LuCl_3$ $I_{Obs.}$
020	0.0174	0.0174	w	0.0176	---	
001	0.0161	0.0159	vs	0.0163	0.0163	vs
110	0.0190	0.0189	mw	0.0191	0.0191	mw
$11\bar{1}$	0.0238	0.0242	mw	0.0239	0.0246	mw
021	0.0335	0.0332	mw	0.0339	0.0339	w
111	0.0464	0.0457	w	0.0469	0.0465	w
130	0.0538	0.0534	vs	0.0543	0.0533	s
$20\bar{1}$	0.0519	0.0534	vs	0.0521	0.0533	s
$13\bar{1}$	0.0586	0.0590	w	0.0591	0.0594	vw
$11\bar{2}$	0.0609	0.0590	w	0.0613	0.0594	vw
040	0.0696	0.0699	w	0.0704	0.0709	vw
$20\bar{2}$	0.0776	0.0763	vw	0.0780	0.0769	vw
131	0.0812	0.0813	vvs	0.0821	0.0820	vs
022	0.0818	0.0813	vvs	0.0828	0.0820	vs
041	0.0851	---		0.0867	0.0867	vw
$13\bar{2}$	0.0956	0.0950	vw	0.0965	0.0986	ms
$22\bar{2}$	0.0950	0.0950	vw	0.0956	---	
201	0.0971	0.0978	ms	0.0981	0.0986	ms
112	0.1060	0.1058	vw	0.1073	0.1073	vw
221	0.1145	0.1147	w	0.1157	0.1156	vw
150	0.1234	0.1220	m	0.1247	0.1239	w
240	0.1280	0.1289	mw	0.1292	0.1298	vw
$15\bar{1}$	0.1282	0.1289	mw	0.1295	0.1298	vw
$31\bar{2}$	0.1324	---		0.1329	---	

TABLE X (continued)

hkℓ	$YbCl_3$ $Sin^2\theta_{Calc.}$	$YbCl_3$ $Sin^2\theta_{Obs.}$	$YbCl_3$ $I_{Obs.}$	$LuCl_3$ $Sin^2\theta_{Calc.}$	$LuCl_3$ $Sin^2\theta_{Obs.}$	$LuCl_3$ $I_{Obs.}$
042	0.1340	0.1365	vw	0.1356	---	
$11\bar{3}$	0.1300	0.1289	mw	0.1313	0.1298	vw
$20\bar{3}$	0.1355	0.1365	vw	0.1365	---	
132	0.1408	0.1422	m	0.1425	0.1428	ms
$24\bar{2}$	0.1472	0.1488	w	0.1484	0.1487	vw
151	0.1508	0.1488	w	0.1525	---	
003	0.1449	---		0.1467	---	
060	0.1566	0.1563	s	0.1584	0.1582	s
$33\bar{1}$	0.1527	---		0.1537	---	
023	0.1623	---		0.1643	---	
$13\bar{3}$	0.1647	---		0.1665	---	
330	0.1705	0.1695	s	0.1719	0.1705	s
061	0.1727	0.1728	s	0.1747	0.1751	s
202	0.1680	0.1695	s	0.1700	0.1705	s
$33\bar{2}$	0.1671	0.1695	s	0.1681	0.1705	s
311	0.1858	0.1864	vw	0.1878	0.1885	vw
$31\bar{3}$	0.1793	---		0.1799	---	
222	0.1854	0.1864	vw	0.1876	0.1885	vw
113	0.1978	---		0.2003	0.2008	vw
$26\bar{1}$	0.2085	0.2102	mw	0.2105	0.2134	mw
$24\bar{3}$	0.2051	---		0.2069	---	
043	0.2145	0.2165	vw	0.2171	---	
400	0.2336	---		0.2352	---	
$26\bar{2}$	0.2342	---		0.2364	---	

TABLE XI

Lattice Constants of $AlCl_3$, YCl_3 and Rare Earth Trichlorides

	$AlCl_3$	YCl_3	$DyCl_3$	$HoCl_3$
a	5.92 A	6.92 A	6.94 A	6.88 A
b	10.22	11.94	11.97	11.90
c	6.16	6.44	6.50	6.41
β	108°	110°20'	111°10'	110°
V	355 A^3	498 A^3	503 A^3	490 A^3
$\frac{b}{a}$	1.726	1.725	1.725	1.730
$\frac{c}{a}$	1.041	0.931	0.937	0.932

	$ErCl_3$	$TmCl_3$	$YbCl_3$	$LuCl_3$
a	6.83 A	6.77 A	6.86 A	6.85 A
b	11.78	11.72	11.69	11.62
c	6.35	6.32	6.53	6.50
β	110°50'	111°	111°30'	111°50'
V	477 A^3	468 A^3	487 A^3	481 A^3
$\frac{b}{a}$	1.730	1.731	1.704	1.696
$\frac{c}{a}$	0.932	0.934	0.952	0.949

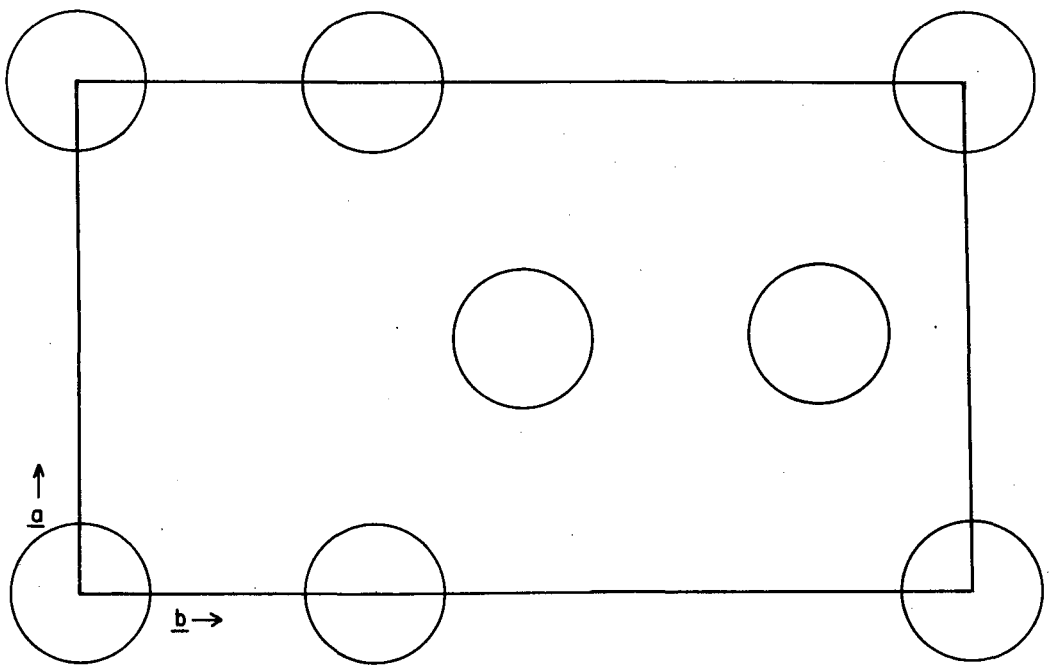

POSITIONS OF YTTRIUM IONS IN TRIAL STRUCTURE

MU3969

Fig. 1

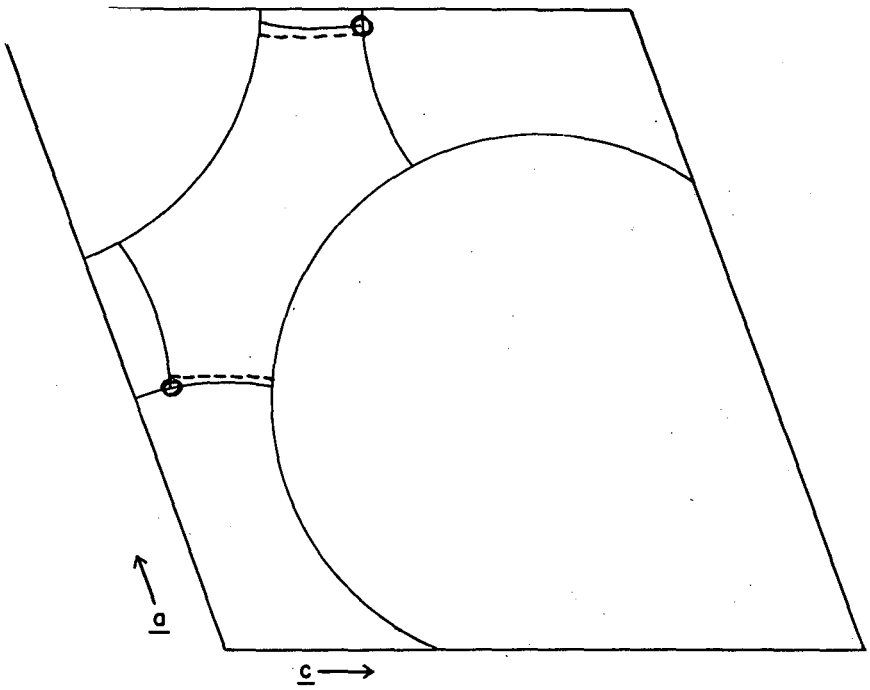

ALTERNATE TRIAL STRUCTURE SHOWING MOST PROBABLE CENTERS OF Cl IONS

MU3970

Fig. 2

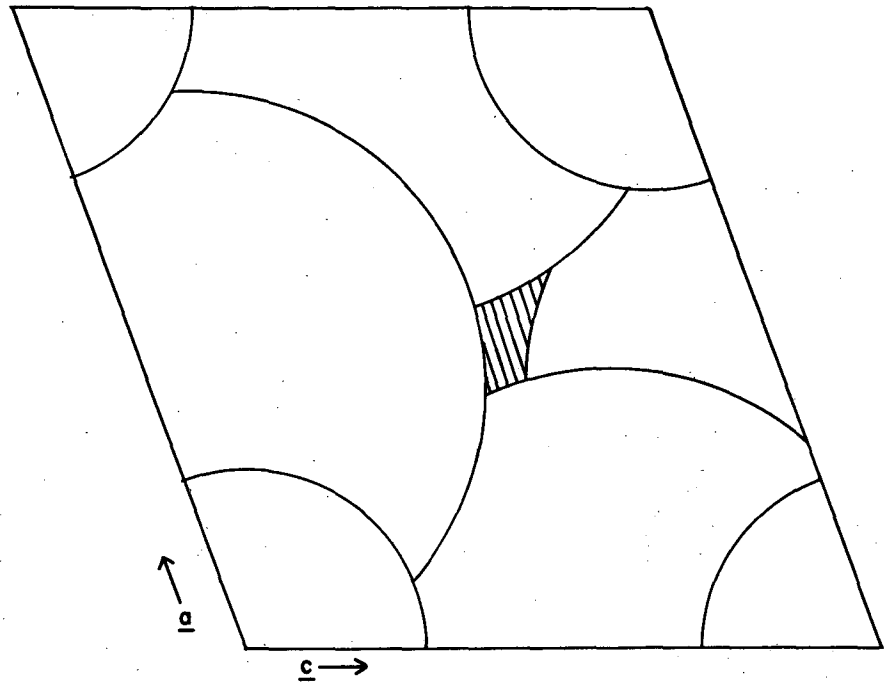

SECOND LAYER OF ALTERNATE TRIAL STRUCTURE

MU3971

Fig. 3

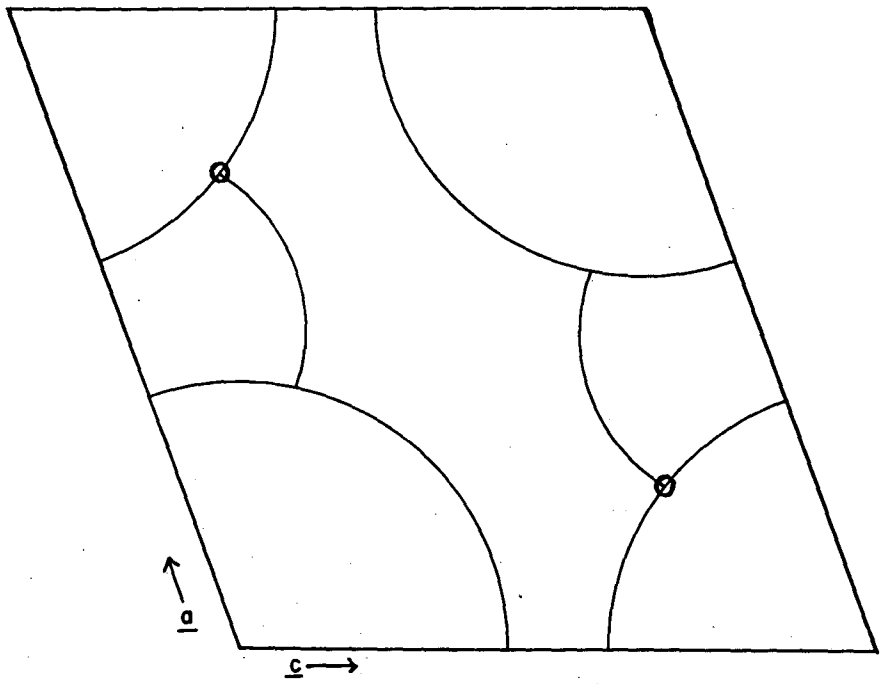

CENTERS OF Cl IONS IN TRIAL STRUCTURE
FIRST LAYER

MU3972

Fig. 4

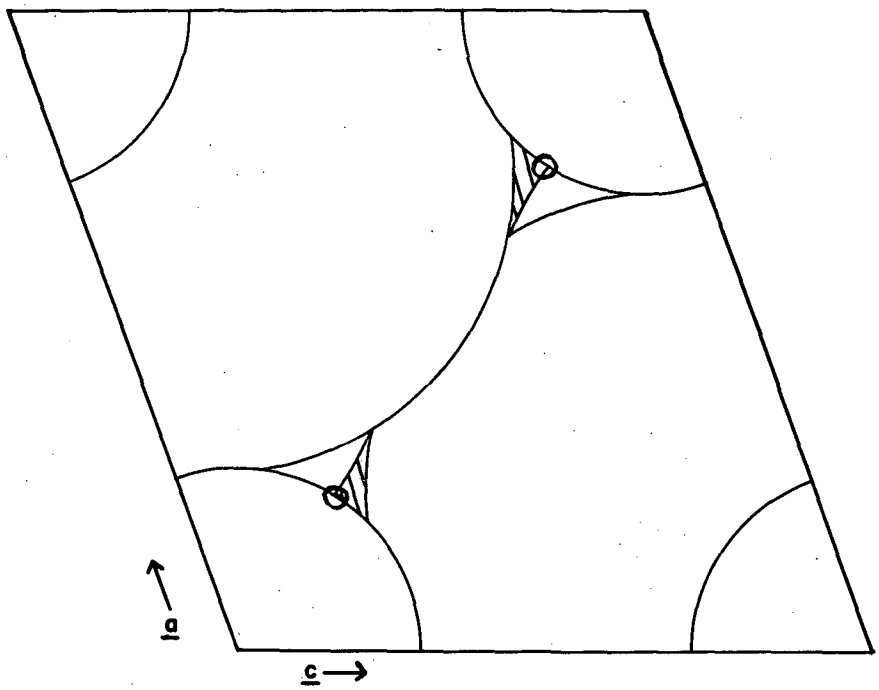

CENTERS OF Cl IONS IN TRIAL STRUCTURE
SECOND LAYER

MU3973

Fig. 5

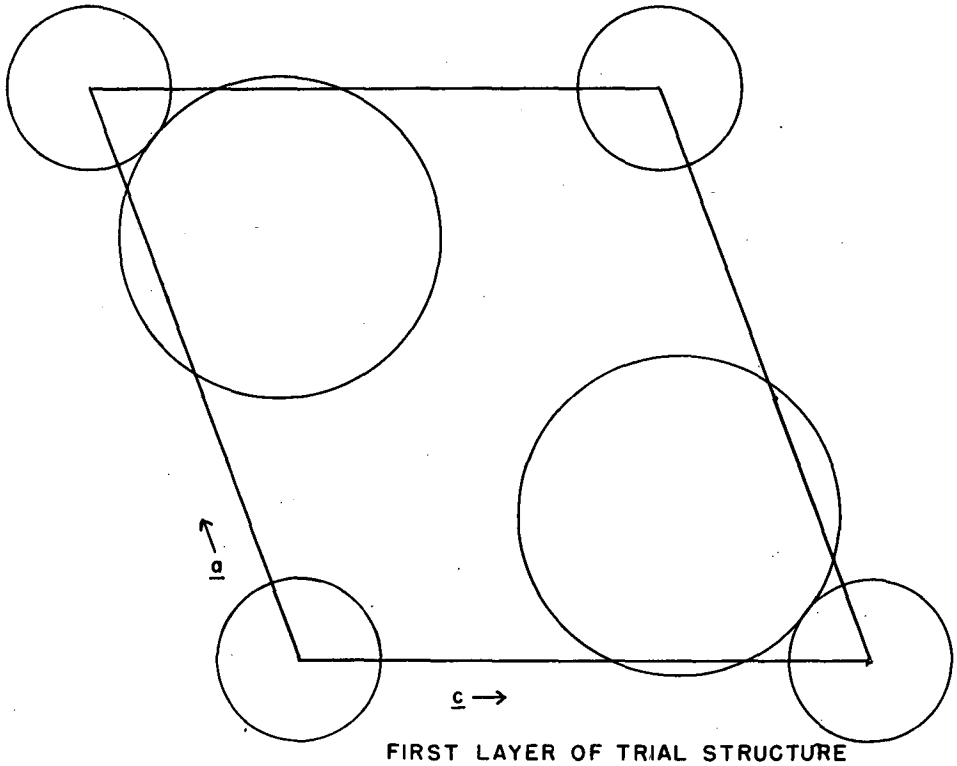

FIRST LAYER OF TRIAL STRUCTURE

MU 3974

Fig. 6

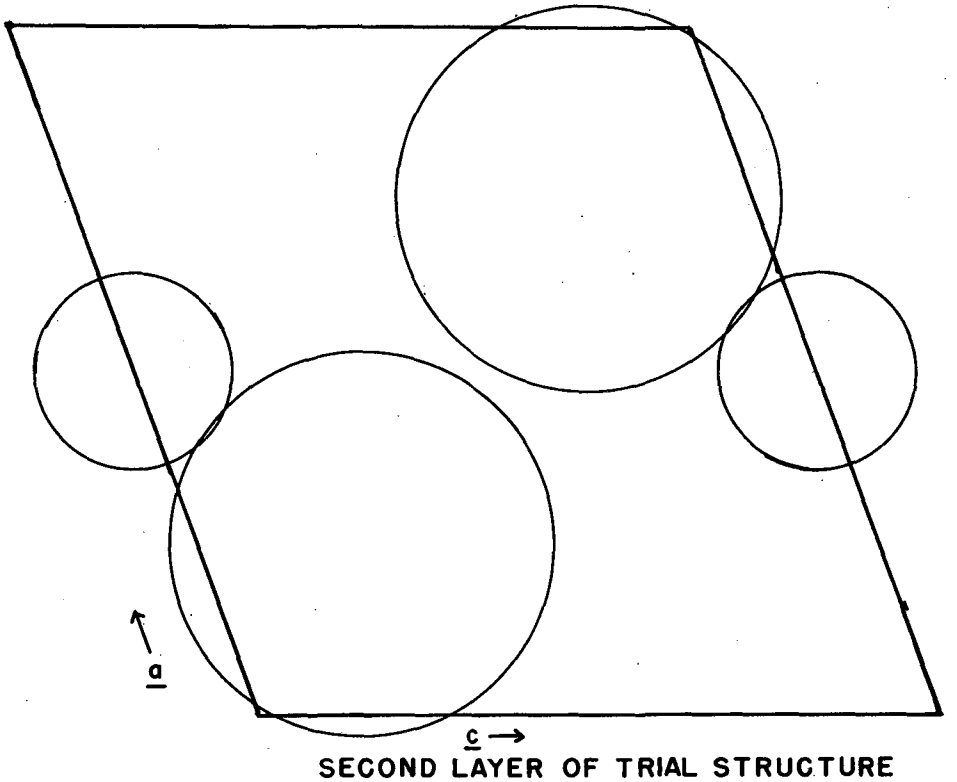

SECOND LAYER OF TRIAL STRUCTURE

MU3975

Fig. 7

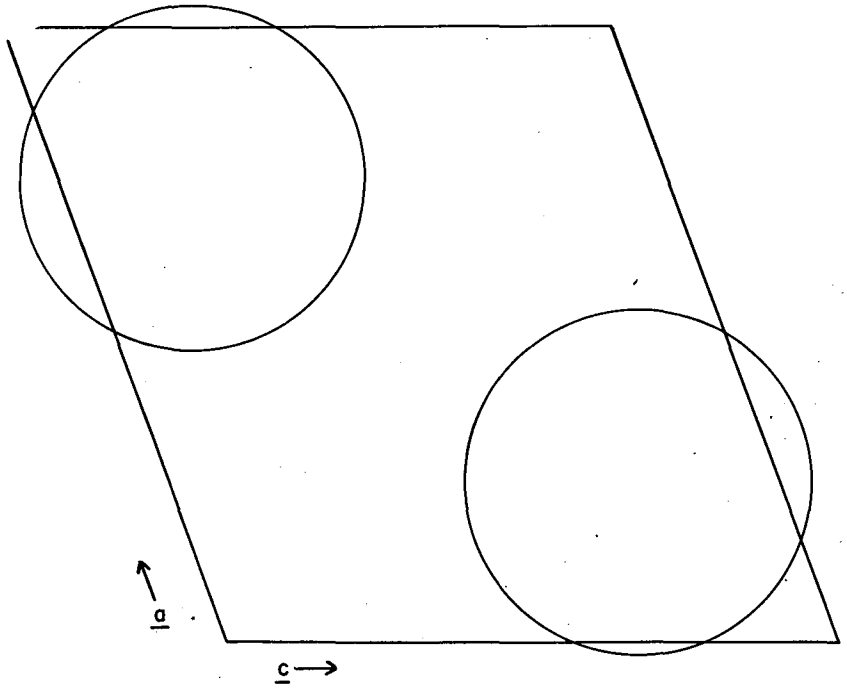

THIRD LAYER OF TRIAL STRUCTURE

MU3976

Fig. 8

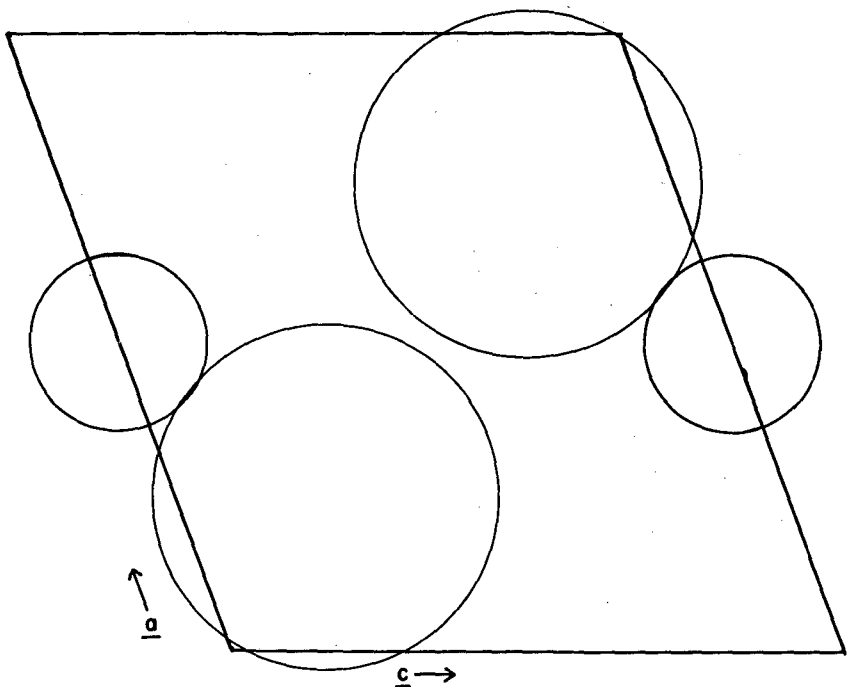

FOURTH LAYER OF TRIAL STRUCTURE

MU3977

Fig. 9

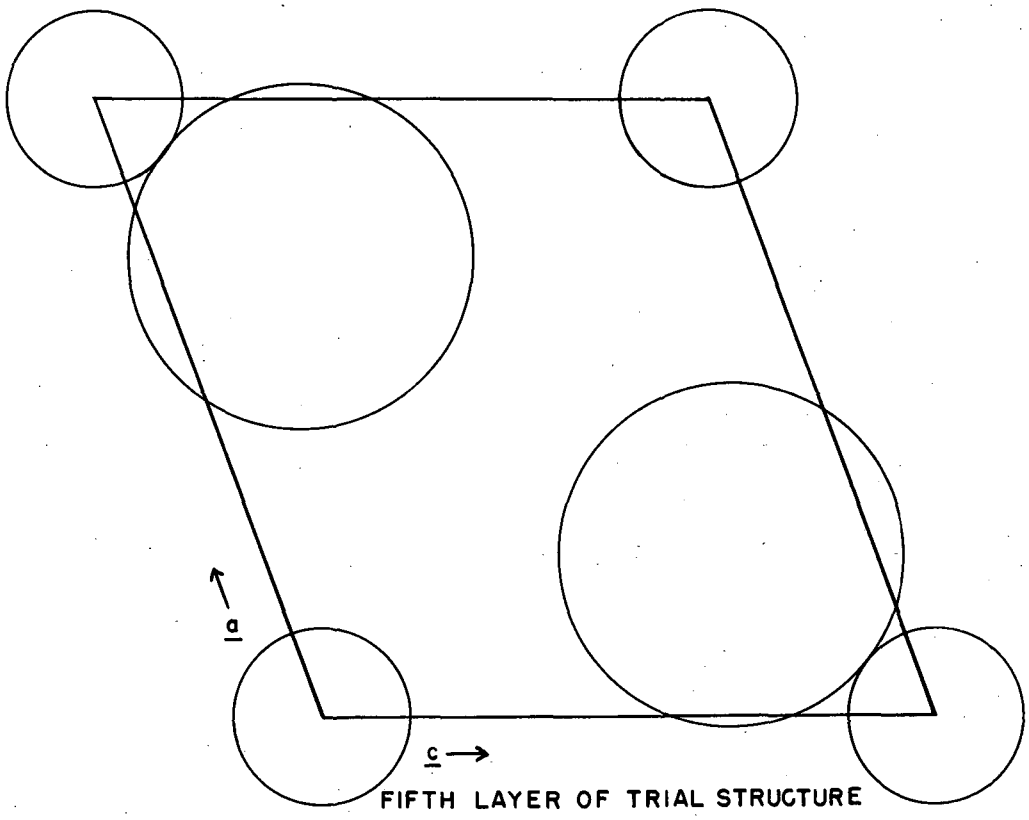

FIFTH LAYER OF TRIAL STRUCTURE

MU3978

Fig. 10

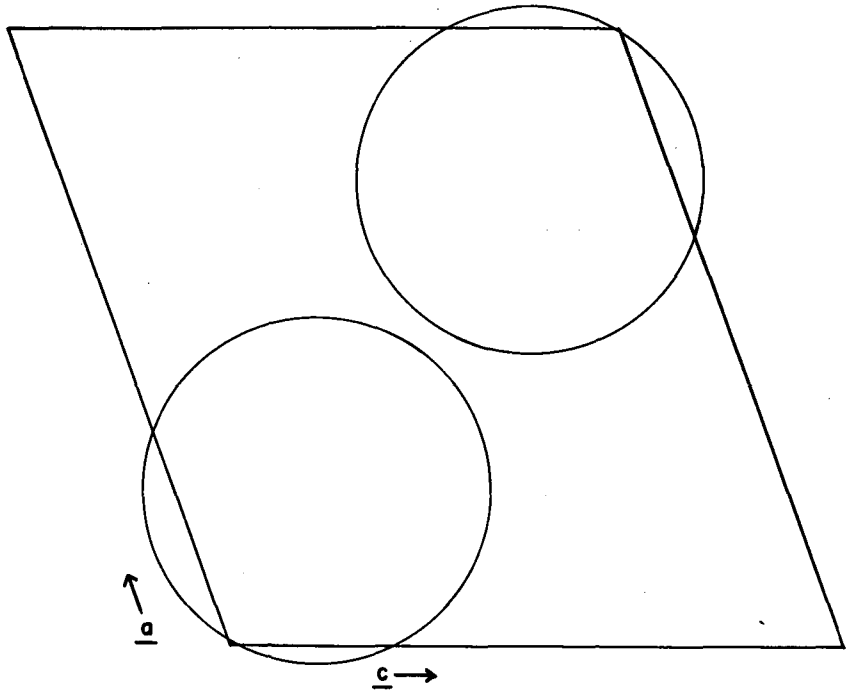

SIXTH LAYER OF TRIAL STRUCTURE

MU3979

Fig. 11

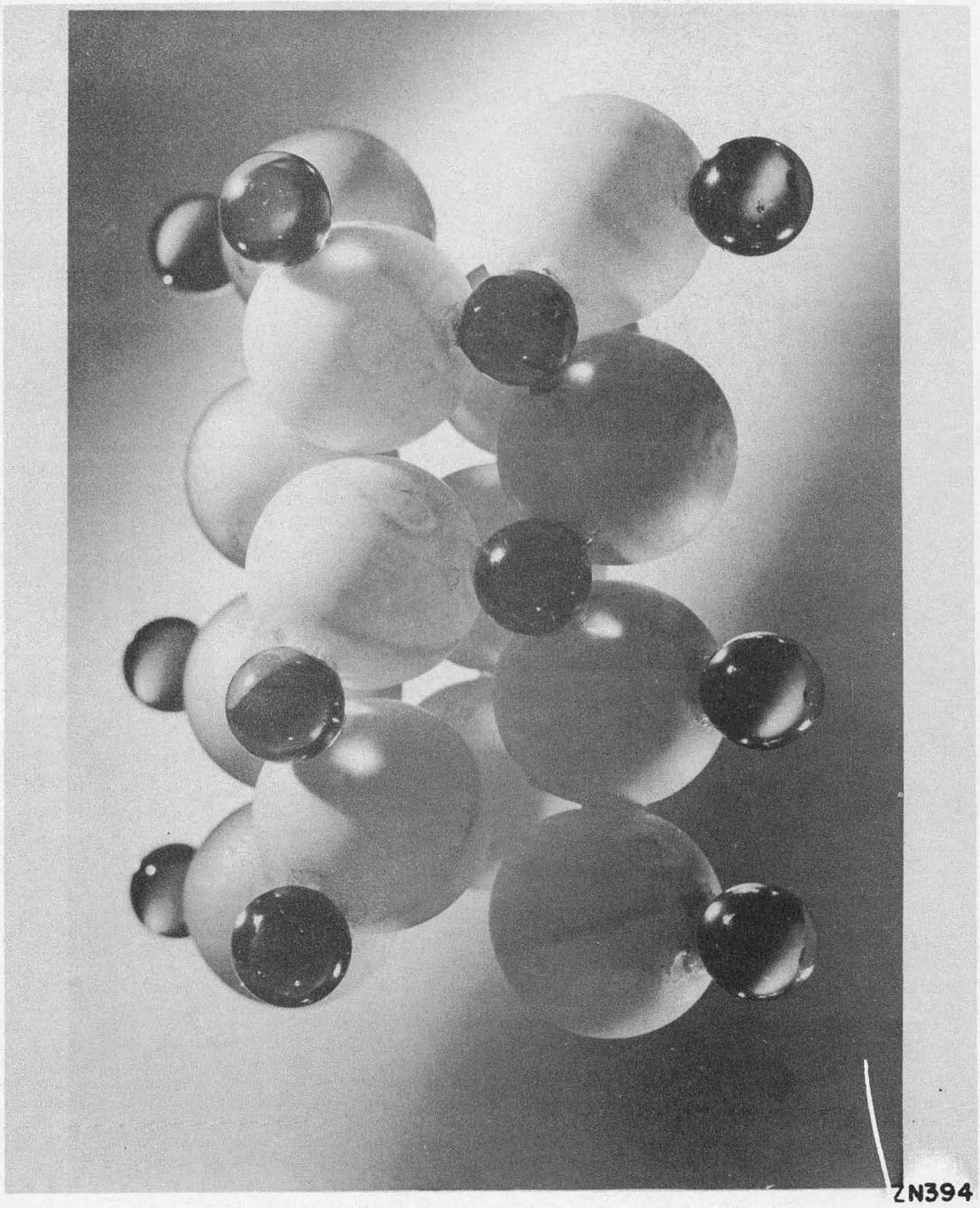

Fig. 12 A-b Plane of Unit Cell of YCl_3

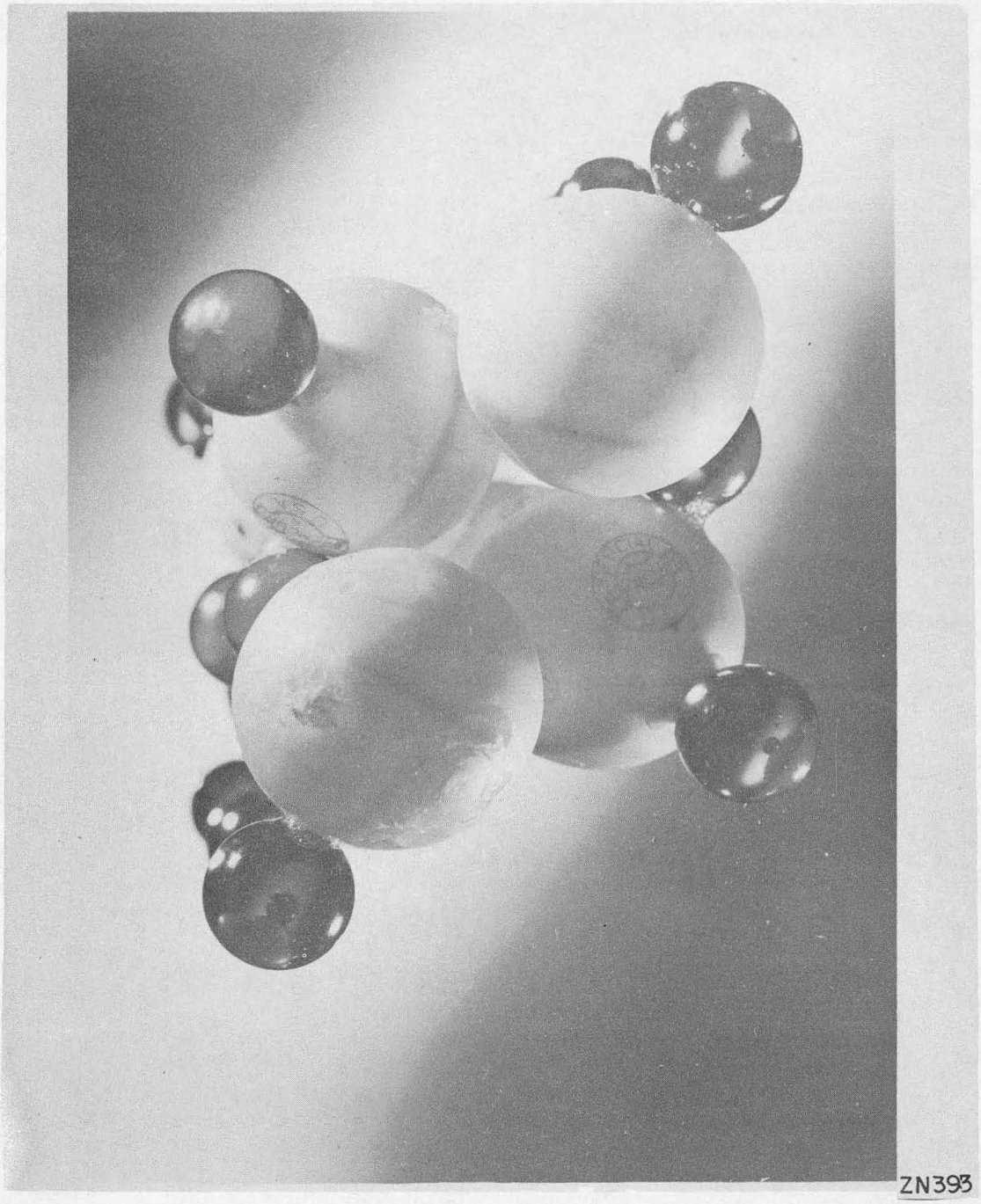

Fig. 13 C-a Plane of Unit Cell of YCl_3